İSTANBUL TECHNICAL UNIVERSITY ★ INSTITUTE OF SCIENCE AND TECHNOLOGY

STRUCTURAL ANALYSIS of STABILIZER BAR UNDER TORSION

M.Sc. Thesis by
E.Mert UYGUN, B.Sc.

Department : **Aeronautical Engineering**

Programme: **Astronautics and Aeronautics Engineering**

JANUARY 2007

İSTANBUL TECHNICAL UNIVERSITY ★ INSTITUTE OF SCIENCE AND TECHNOLOGY

STRUCTURAL ANALYSIS of STABILIZER BAR UNDER TORSION

M.Sc. Thesis by

E. Mert UYGUN, B.Sc.

(511031030)

Date of submission : **25 December 2006**

Date of defence examination: **24 January 2007**

Supervisor (Chairman): **Assoc. Prof. Dr. Metin O. KAYA**

Members of the Examining Committee **Prof.Dr. İbrahim ÖZKOL (İTÜ.)**

Assoc.Prof.Dr. Erol UZAL (İÜ.)

JANUARY 2007

<u>İSTANBUL TEKNİK ÜNİVERSİTESİ ★ FEN BİLİMLERİ ENSTİTÜSÜ</u>

YÜK ETKİSİNDEKİ STABİLİZATÖR ÇUBUĞUN YAPISAL ANALİZİ

Master Tezi

E.Mert UYGUN

(511031030)

Tez teslim tarihi : 25 Aralık 2006

Tez savunma sunumu tarihi : 24 Ocak 2007

Danışman (Sunum başkanı): Doç. Dr. Metin O. KAYA

Tez Savunma Sunumu Kurul Üyeleri : Prof.Dr. İbrahim ÖZKOL (İTÜ.)

Doç.Dr. Erol UZAL (İÜ.)

OCAK 2007

PREFACE

My Thesis "Structural Analysis of Stabilizer Bar under Torsion" was a major work which would be not possible without the help of many. Therefore my special thanks go to:

- Mercedes-Benz Turk Co. for keeping a high standart of acedemic quality even on production and in particular to Development Bus department allowing me to prepare my master thesis at their facilities;

- M.Sc.Fatih Öncel for his great help with my numerous technical questions and providing me with the test results whenever I asked for;

- My adviser Assoc.Prof.Dr. Metin O.Kaya for his continuos support and input for valuable ideas.

Aralık, 2006 E.Mert Uygun

TABLE OF CONTENTS

TABLE LIST

Page Nr

FIGURE LIST

YÜK ETKİSİ ALTINDA STABİLİZATÖR ÇUBUĞUN YAPISAL ANALİZİ

ÖZET

Stabilizatör çubuklar süspansiyon sistemlerinin emniyet segmentlerinden olup, periyodik ve büyük statik yüklere maruz kalan bileşenlerdir. Hafif konstuksiyonların gereksinimlerini karşılamak durumundadırlar. Bu ancak iyi tasarlanmış çubukların yüksek dayanımlı ve özel malzemeler kullanılarak dikkatli bir şekilde imal edilmesi ile mümkün olabilir. İmal süreçlerinde başvurulacak bazı ek özel yöntemler, yüzeydeki gerilimin azaltılması konusunda avantaj sağlayabilir. Yük altındaki çubukların imalinde sağlanacak her türlü iyileştirme, sözkonusu yüzey gerilimini asgari düzeye indirgemeyi hedeflemektedir.

Tez başlangıcında yeralan ve yorulma konusu ile ilişkili teorik açıklamalar içeren bölümlerden sonra stabilizatör parça kısaca tanıtılmaktadır, sonrasında ise farklı malzemeler kullanılarak imal edilen ve yüzey sertleştirme tekniğiyle mukavemetlendirilen numune parçalar karşılaştırılmalı olarak değerlendirimektedir. Bu numunelerin yük altındaki davranışı deney ortamında defalarca test edilerek raporlanmıştır. Değişik tedarikçilerden temin edilen numuneler ayrı ayrı teste tabii tutulmuş ve toplanan veriler numune bazında kaydedilmiştir.

Deney sonuçları yine ayrı ayrı tablolara işlenmiş ve bu matematiksel verilerin grafiksel olarak ifade edilmesine çalışılmıştır. S-N Eğrileri (literatürde Wöhler Eğrileri olarakta bilinmektedir) hangi numunenin daha mukavim olduğunu açıkça göstermektedir. Eğrilerin altında kalan alan büyüdükçe numunenin yük altında daha başarılı bir performans gösterdiği ve dolayısıyla hangi tedarikçinin imal yöntemlerinin daha etkin olduğu anlaşılır.

Mekanik özelliklerinin yanısıra hammaddeleri de iyileştirilen numune parçalar hakkındaki tüm deneysel sonuçlar ve kimyasal bilgiler A ve B eklerinde ayrıntılı olarak yer almaktadır.

Deneysel sonuçlarla yetinilmemiş ve ANSYS adı verilen analiz programı yardımı ile (FEM - Sonlu Elemanlar Yöntemi kullanılarak analiz yapan özel bir yazılımdır) matematiksel bir yaklaşımda da bulunulmuştur. ANSYS yazılımı ile stabilizatör çubuğunun büküm noktalarında ve diğer bazı kritik bölgelerinde yük altında tecrübe edilecek eşdeğer gerilim/gerinim hesapları hassas bir şekilde gerçekleştirilmektedir. Hesaplanan değerler katı model üzerinde farklı renkler ile ifade edilir. Deforme olmayan alanlar mavi renkle işaretlenirken, hasarlanması olası bölgeler taşıdığı riske oranla kırmızı renge doğru dönecektir.

ANSYS analizleri tamamlandığında edinilen sonuçlar tezin son kısmında deneysel veriler ile de karşılaştırılmış ve yaklaşımın gerçeği yansıttığı kanıtlanmıştır. Metinde yer almayan bazı ayrıntılı grafikler ve matematiksel veriler C ekindedir.

Teorik Yöntemler kısmında geçen teknik açıklamalar tez ile ilgili aşağıdaki anahtar kelimeleri içermekte bazı temel konulara ışık tutmaktadır:

„Yorulma, Gerilme, Poisson Oranı, Kayma gerilmesi, Gerinme, Plastik deformasyon, Süneklik, Gerilim-Gerinim Eğrileri, Yüzey Sertleştirme, Sonlu Elemanlar Yöntemi, ANSYS, Süspansiyon sistemi, Şasi".

STRUCTURAL ANALYSIS OF STABILIZER BAR UNDER TORSION

SUMMARY

Stabilizer bars belong to the components with the highest cyclic and superposed static load and are the security segments of the suspension system. They have to fulfill the requirements of lightweight constructions. This is only possible, if high strength materials with special properties are carefully manufactured to well designed roads and special additional treatments are carried out, which impose a advantageous residual stress profile in the surface layers of the roads.

After a short theoretical view on the technical terms related to the fatigue topic, some aspects of the fatigue behavior of the stabilizer bars are presented. Then the fatigue properties of shot peened specimens made of different materials are discussed. Finally some results on the fatigue behavior of different kind of specimens at a very high number of load cycles are reported.

During the experiments taken values are listed at some tables and after their evaluation the results are depicted on the graphs. S-N Curves (also known as Wöhler Curves) and shows the durability of different specimens and give the clue which company has succeeded producing the most lasting bar.

Comparison tables of overall measurements and chemical properties of raw materials are added to the Appendix sections A and B.

Experiment results are also supported with ANSYS – FEA calculations, which are representing a different aspect. This mathematical approximation is made through those measurements in order to calculate the maximum equivalent stress values on the bends and possible fracture points on these meshed surfaces are indicated where the blue color turns into red.

After analyzing with ANSYS software experiment results have been also verified with the computer calculated ones and an appendix section is made (App.C) to show the fatigue behavior of metal in graphs.

All technical terms used in this work are collected and explained under header "Theoretical Methods" at Section 3. Following terms will help to understand the topic better:
Fatigue, Tensile stress, Poisson's ratio, Shear stress, Tensile strength, Yield strength, Plastic deformation, Ductility, Ductile material, Stress-Strain Curve, Strain hardening, Residual stresses, Peening, Shot peening, Stiffness, the S-N Curve, FEA (Finite Element Analysis, ANSYS, Car suspensions, Chassis.

1 INTRODUCTION

Stabilizer bars belong to the components with the highest cyclic and superposed static load and are the security segments of the suspension system. They have to fulfill the requirements of lightweight constructions. This is only possible, if high strength materials with special properties are carefully manufactured to well designed roads and special additional treatments are carried out, which impose a advantageous residual stress profile in the surface layers of the roads.

After a short theoretical view on the technical terms related to the fatigue topic, some aspects of the fatigue behavior of the stabilizer bars are presented. Then the fatigue properties of shot peened specimens made of different materials are discussed. Finally some results on the fatigue behavior of different kind of specimens at a very high number of load cycles are reported.

During the experiments taken values are listed at some tables and after their evaluation the results are depicted on the graphs. S-N Curves (also known as Wöhler Curves) and shows the durability of different specimens and give the clue which company has succeeded producing the most lasting bar. Comparison tables of overall measurements and chemical properties of raw materials are added to the Appendix sections A and B.

Experiment results are also supported with ANSYS – FEA calculations, which are representing a different aspect. This mathematical approximation is made through those measurements in order to calculate the maximum equivalent stress values on the bendings and possible fracture points on these meshed surfaces are indicated where the blue color turns into red.

1.1 KEYWORDS

All technical terms used in this work are collected and explained under header "Theoretical Methods" at Section 3. Following terms will help to understand the topic better:

Fatigue, Tensile stress, Poisson's ratio, Shear stress, Tensile strength, Yield strength, Plastic deformation, Ductility, Ductile material, Stress-Strain Curve, Strain hardening, Residual stresses, Peening, Shot peening, Stiffness, the S-N Curve, FEA (Finite Element Analysis, ANSYS, Car suspensions, Chassis.

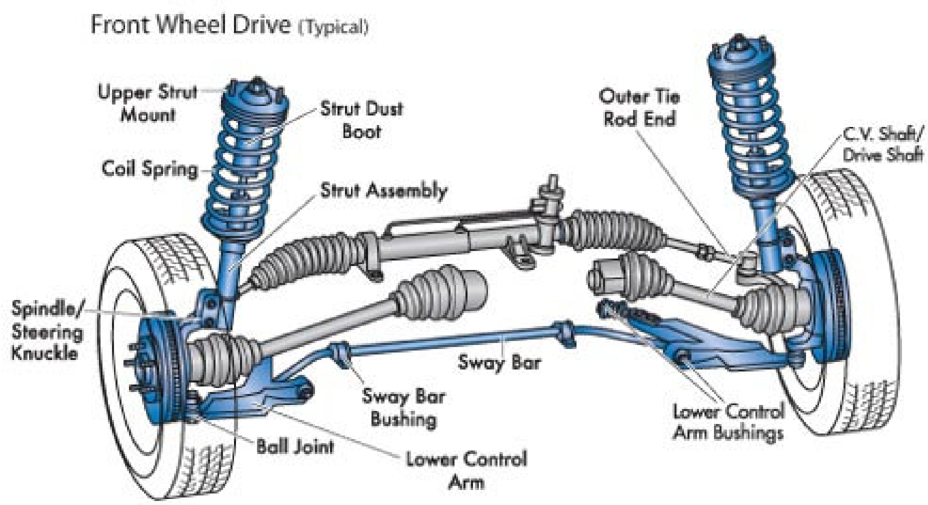

Figure 1.1: Drawing of the front suspension system. Stabilizer bar also called as the Sway Bar or Anti-Roll Bar. On this sample, parts of the car suspension and sway bar itself are clearly seen (Thumbnail is taken from the web site: www.turbosquid.com).

1.2 STABILIZER BAR

The expression "Stabilizer Bar" represents an important component of the suspension system in an arc shape and having a duty of security function, which mostly is required to have some main properties in common: great range of elastic loading, high strength and satisfactory ductility, high resistance against fatigue failure as well as against setting.

The front wheel support arms are connected by a stabilizer bar, as are the rear wheels (See Fig.1.1). Following any changes in load this bar reestablishes the balance of the suspension, by being twisted. In other words, if four people get into the car, the weight increase makes the stabilizer bar rotate to make the car hold onto its normal position.

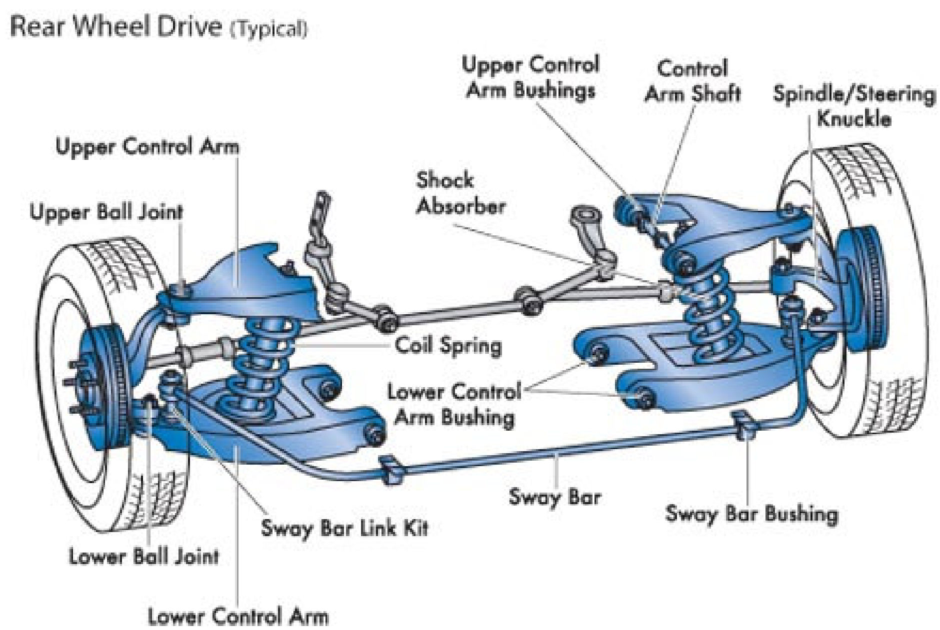

Figure 1.2: Drawing of the rear suspension system. This Sway Bar (Stabilizer Bar) is much longer than the one at the front (Thumbnail is taken from the web site: www.turbosquid.com).

1.3 HOW DO STABILIZERS WORK ?

Stabilizer bars are part of a car's suspension system and are located both on the front and back sides of the car (See Fig.1.1 and 1.2). They are sometimes also called anti-sway bars or anti-roll bars. Their purpose in life is to try to keep the car's body from "rolling" in a sharp turn.

Inside the car having a sharp turn, passenger bodies get pulled toward the outside of the turn. The same thing is happening to all the parts of the car. So the part of the car on the outside of the turn gets pushed down toward the road and the part of the car on the inside of the turn rises up.

In other words, the body of the car "rolls" toward the outside of the turn. If the speed is fast enough, the tires on the inside of the turn actually rise off the road and the car flips over.

Rolling tends to put more weight on the outside tires and less weight on the inside tires, while reducing traction and steering also. The body of the car shall remain flat through a turn so that the weight stays distributed evenly on all four tires.

A “Stabilizer bar” tries to keep the car's body flat by moving force from one side of the body to another. A stabilizer bar is like a metal rod that is having about 2 to 5 cm in diameter, which is attached to the frame of the car in front of the front tires with bushings, in case that it rotates on its own. However their arms are attached to the front suspension member on both sides (See Fig.1.3).

While going into a turn now, the front suspension member of the outside of the turn gets pushed upward. The arm of the stabilizer bar gets pushed upward, and this applies torsion to the rod.

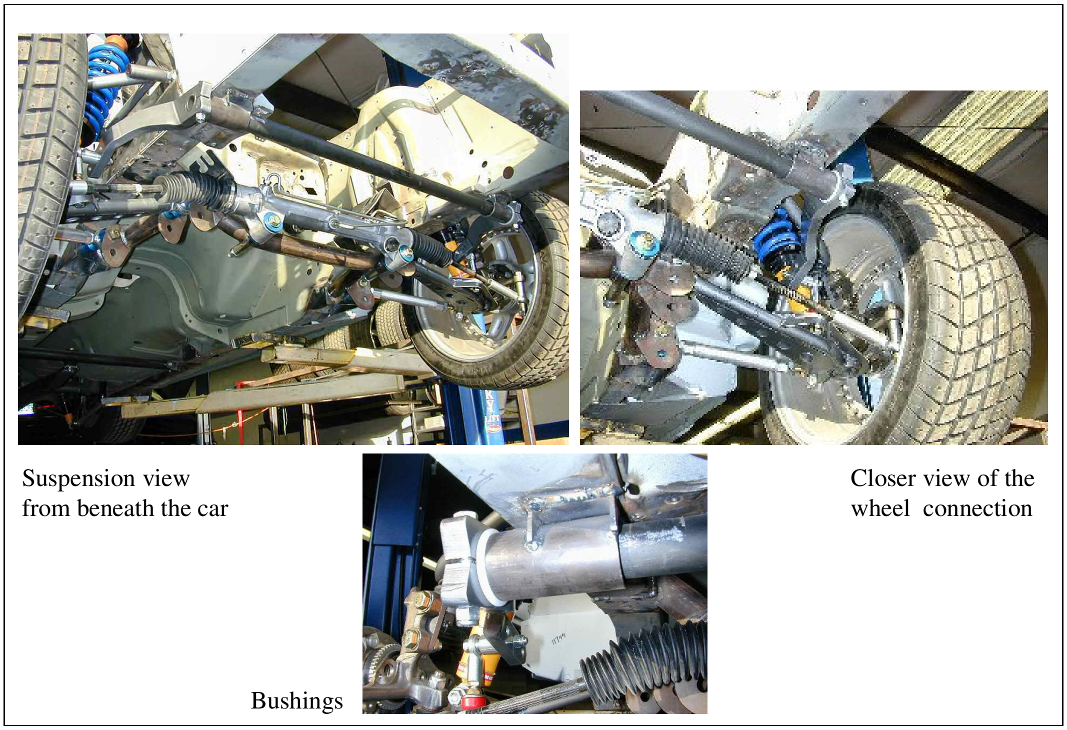

Figure 1.3: Suspension system mounted on chassis (personal car). Attached on both of the axis ends and also fixed with bushings.

The torsion them moves the arm at the other end of the rod, and this causes the suspension on the other side of the car to compress as well. The car's body tends to stay flat in the turn.

Without having a stabilizer bar, it is likely possible experiencing a body roll in a turn. By the way, having the stabilizer bar more than needed causes losing independence between the suspension members on both sides of the car. When one wheel hits a bump, the stabilizer bar transmits the bump to the other side of the car as well, which is not acceptable. The ideal is to find a setting that reduces body roll but does not hurt the independence of the tires.

Stabilizer bars are usually estimated as simple components. But recent requirements for a great number of stabilizer bars, applied in constructions for cars or buses, can only be met if high strength materials with special properties are carefully manufactured to well designed rods and furthermore additional treatments are carried out.

Especially shot peening method is very important and efficient treatment to improve the fatigue properties of stabilizers to the necessary level. The pic a shot peening process is showed below at the Figure 1.4.

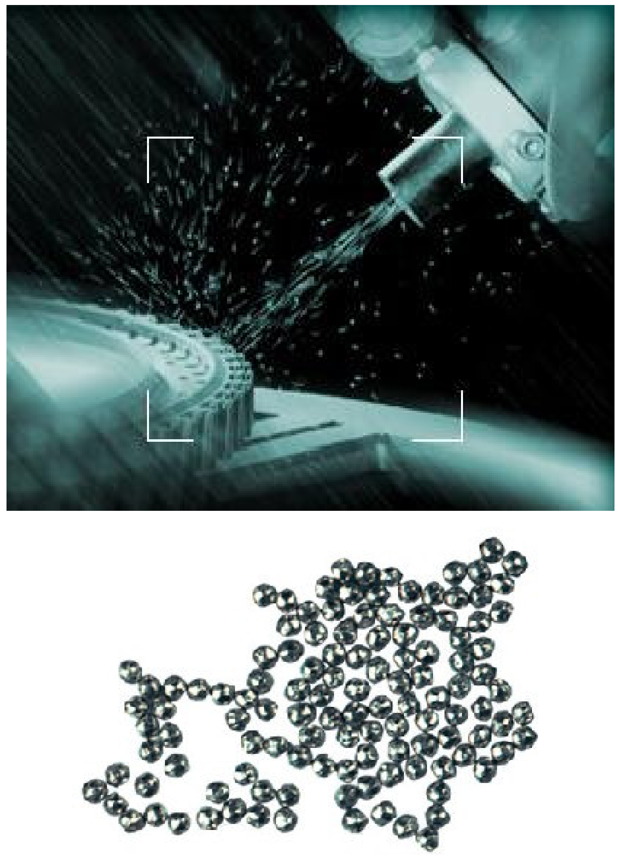

Figure 1.4: Shot peening process and spherical conditioned cut wire. See Theoretical Methods for more details.

In this paper the importance of stabilizer bars is stated for the suspension system. Problems of stabilizer bars likely appear as fatigue failures or as plastic deformations (setting). Fatigue fractures during vehicle operation initiate at points, where local stresses exceed the fatigue strength. Those dangerous locations are determined by the shape of the bar. Stabilizers compensate especially high stresses at the bendings and at the interior zone of the surfaces.

Numerous fatigue tests on different torsional specimens are performed for this thesis and all these specimen are tested with the help of Hydropuls testing machine [a,*].

1.4 The PURPOSE of TEST

The test yields characteristics, from which the mechanical behaviour of materials or structural elements under constant or repeated pulsating or alternating loading can be derived. It is termed a continuous vibration test (short: fatigue test), because the loading at the specimen is applied in form of vibration [12].

---

a. See: Part 4 : Experimental Methods, Hydropuls Testing Machine
[12]: DIN 50100, Continuous Vibration Test Standart

2 PQF REPORTS

Figure 2.1: 3D Drawings for City Bus (3D models are downloaded from the web site : www.turbosquid.com).

After Sales Services regularly make statistics about the failure frequency of spare parts while obtaining the data from the authorized technical services worldwide. In the range of "Quality Assurance" issues PQF Reports are used to evaluate the suitable data. PQF stands for "Portable Questionnaire Format" which is a type of an electronic form and auto collation software to manage data acquisition and results collation from the source.

Stabilizer bars, as the main topic of this work, have been reported by technical employees as followed.

PQF Reports below have been prepared for a city bus model (See Fig.2.1) used at a municipal bus line in South America.

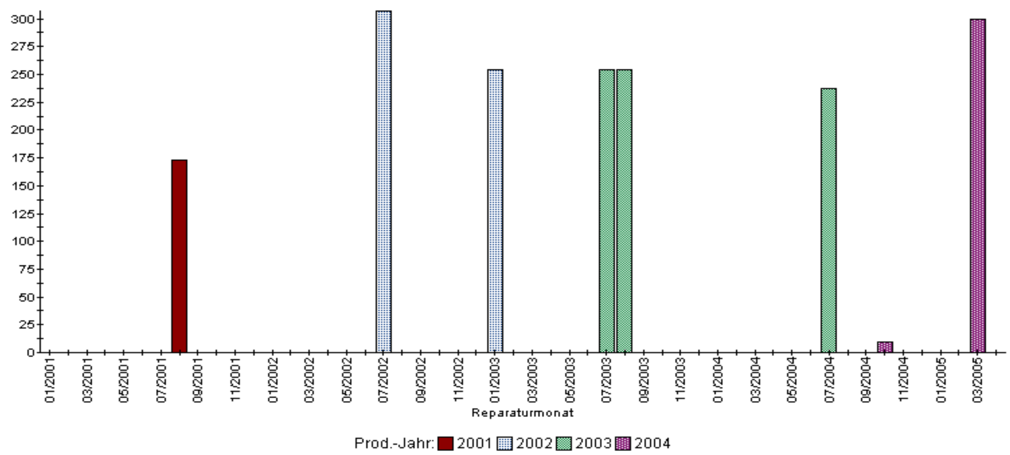

Figure 2.2: Costs in € per Month and Year of Production

At Figure 2.2, costs of the repairments are depicted related to the prices of the Table 2.1. They are also shown distributed over five production years in order to follow the failures precisely which are occurring in a certain time period.

Table 2.1: Values distributed over the years related Fig.2.2

	2001	2002	2003	2004
Repair in 2001	173	0	0	0
Repair in 2002	0	307	0	0
Repair in 2003	0	254	508	0
Repair in 2004	0	0	237	10
Repair in 2005	0	0	0	300

The number of part failures remarkably increasing by vehicles produced in the year 2002 and 2003 where the costs rising high. Especially some columns as seen on the graph (See Fig.2.2) are reaching the level of 250 T € and 300 T € level at some months of past three years.

As a consequence of these part failures, insurance payments and workshop costs are rising higher and the producers profits are put under threat.

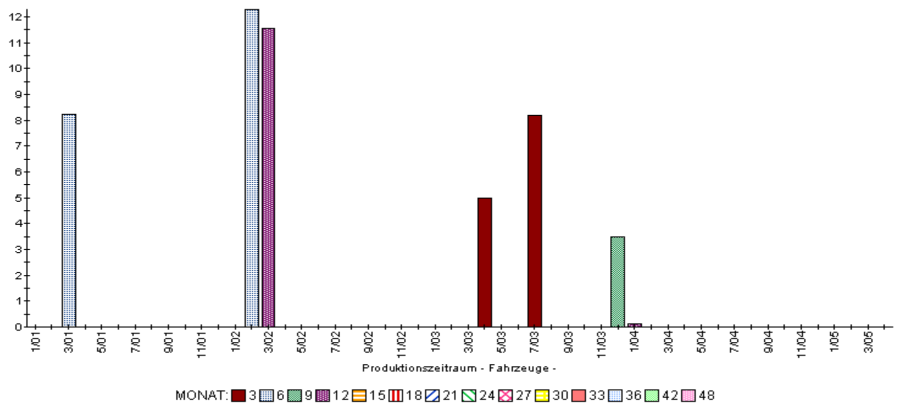

Figure 2.3: Cost in € / produced vehicle at the same year

Repair costs from an another point of view (distributed over months) have been shown on the Figure 2.3 above. In the first quarter of the year 2002 costs are clearly increasing again.

PQF Reports help doing strategically planning by recording scientific and other research data like customer feedbacks depicted at the graphics in order to assure customer satisfaction. These audits and reviews are also financially defending producers outcome.

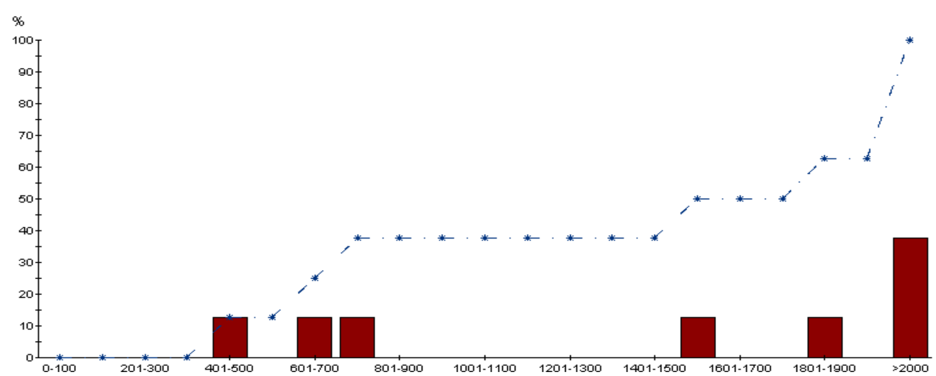

Figure 2.4: Failure distribution through destination

Columns at Figure 2.4 above in dark red color represent Relative Frequency of Failure and blue dots donate Cumulative values.

Figure 2.5: Interurban Bus - 3D Drawing (3D models are downloaded from the web site : www.turbosquid.com).

As a second review, graphs below (See Fig.2.6, 2.7 and 2.8) are mentioning about the part failures and repair costs of interurban bus models (See Fig.2.5).

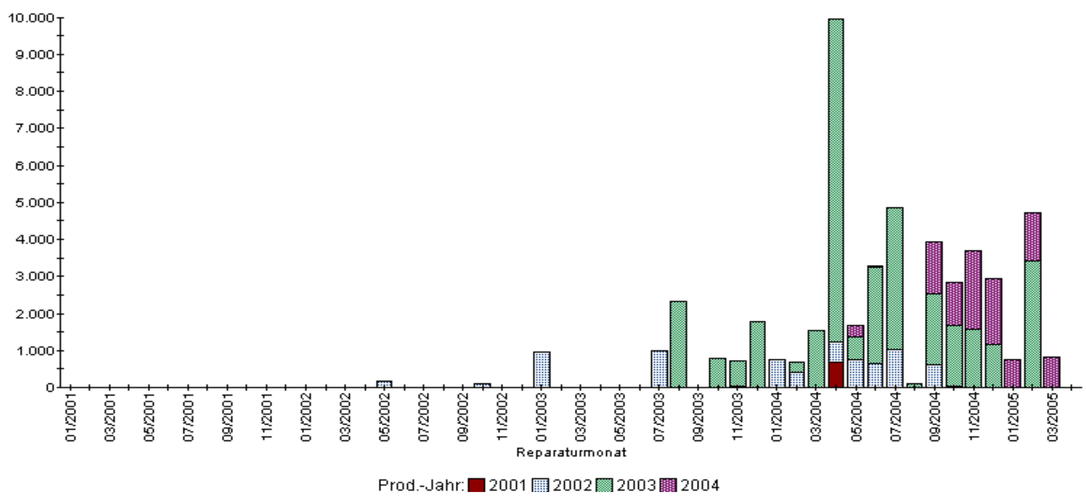

Figure 2.6: Costs in € per Month and Year of Production

Green columns in the Figure 2.6 are depicting that the parts mostly produced in the year 2003 have contributed highly costs in the past three years. The failures have frequently occurred in the second and third quarters of the year 2004. Cumulative costs over past four years can be followed at the Table 2.2, which is representing the source data of the Figure 2.6.

Table 2.2: Values distributed in years related Fig.2.2

	2001	2002	2003	2004
Repair in 2001	0	0	0	0
Repair in 2002	0	247	0	0
Repair in 2003	0	1994	5566	0
Repair in 2004	680	4842	23929	6761
Repair in 2005	0	0	3419	2878

According the same logic of the former graphs, costs per time data of interurban buses are presented as followed. Results are apparently alike, because the concentration of the colored boxes point out that the failure costs at the year 2003 are the highest comparing the data by other time periods (See Fig.2.7).

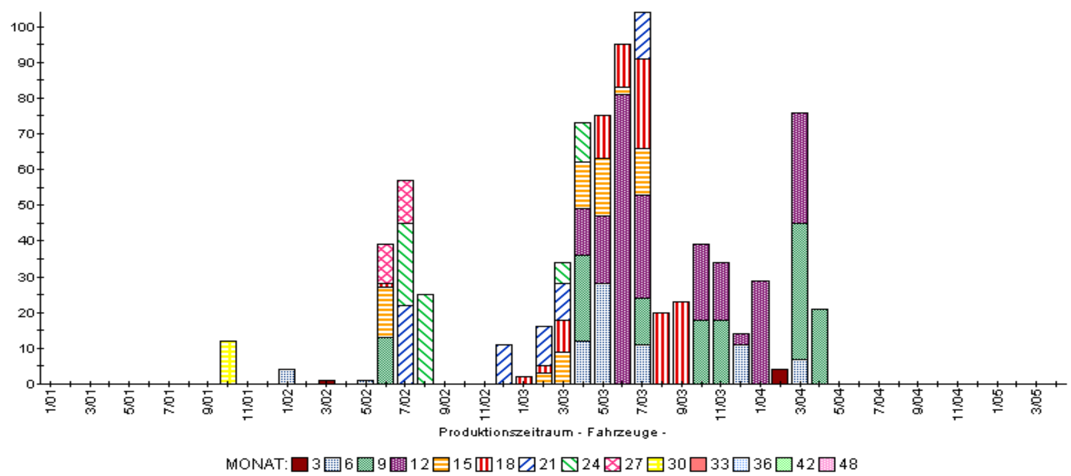

Figure 2.7: Costs in € per Month and Year of Production

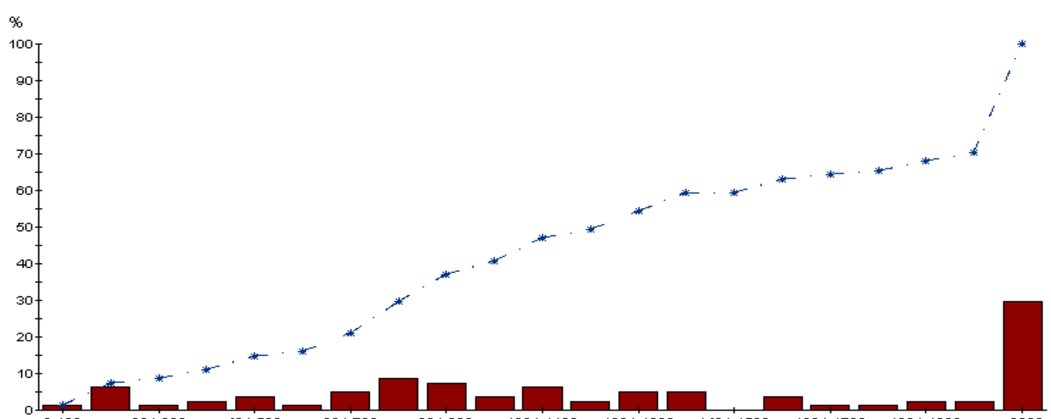

Figure 2.8: Failure distribution through destination

Columns at Figure 2.8 in dark red color represent Relative Frequency of Failure and blue dots donate Cumulative values. Here is also seen that the destination is another important parameter which can not be neglected doing cost reviews.

The recorded data at the former example (See.Fig.2.4) was also showing that the failure rate is increasing by destinations over 2.000.000 km and more, which could be easily achieved through routine cycles of buses. However it is also remarkable that the failure rate makes a peak nearly 1.000.000 km. According these scattered values that the curve contains at Figure 2.4, it could be argued about milestones at each million (as km), where the failure ratings are increasing.

PQF Reports are delivering results ready for analysis. After Sales Services indicated that Stabilizer bars must be optimized in order to decrease the costs of insurance payments and other. Because that these parts are manufactured by different suppliers, this problem is passed on the Development department as a technical issue passed, where the engineers must contact the suppliers in order to solve the difficulties experienced by that parts. Related suppliers mentioned at this thesis are presented with nick names like Co. A, B and C in order to keep their works confidential in the matter of Corporate Identity.

3 THEORETICAL METHODS

This part includes specific terms related to the fatigue behaviour, which were frequently used during the thesis. In order to explain technical facts, the following (bold written headers) will come in very useful.

3.1 CHARACTERISTICS of FATIGUE FAILURES

The following characteristics are common to fatigue in all materials:

1. The process starts with a microscopic crack, called the initiation site, which then widens with each subsequent movement, a phenomenon analysed in the topic of fracture mechanics.
2. Failure is essentially probabilistic. The number of cycles required for failure varies between homogeneous material samples. Analysis demands the techniques of survival analysis.
3. The greater the applied stress, the shorter the life.
4. Damage is cumulative. Materials do not recover when rested.
5. Fatigue life is influenced by a variety of factors, such as temperature and surface finish, in complicated ways.
6. Some materials (e.g., some steel and titanium alloys) exhibit an endurance limit or fatigue limit, a limit below which repeated stress does not induce failure, theoretically, for an infinite number of cycles of load. Most other non-ferrous metals (e.g., aluminium and copper alloys) exhibit no such limit and even small stresses will eventually cause failure.

7. As a means to gauge fatigue characteristics of non-ferrous and other alloys that do not exhibit an endurance limit, a fatigue strength is frequently determined, and this is typically the stress level at which a component will survive 10^7 loading cycles.

Shortly in other words:

3.2 FATIGUE

In materials science, fatigue is the progressive, localized, and permanent structural damage that occurs when a material is subjected to cyclic or fluctuating strains at nominal stresses that have maximum values less than (often much less than) the static yield strength of the material. The resulting stress may be below the ultimate tensile stress, or even the yield stress of the material, yet still cause catastrophic failure [2]: **Russell A. Chernenkoff, John J. Bonnen,** 1997.

3.3 TENSILE STRESS

Tensile stress (or tension) is the stress state leading to expansion; that is, the length of a material tends to increase in the tensile direction. The volume of the material stays constant. Therefore in a uniaxial material the length increases in the tensile stress direction and the other two directions will decrease in size (Poisson's ratio). In the uniaxial manner of tension, tensile stress is induced by pulling forces across a bar, specimen, etc. Tensile stress is the opposite of compressive stress.

Structural members in direct tension are ropes, soil anchors and nails, bolts, etc. Beams subjected to bending moments may include tensile stress as well as compressive stress and/or shear stress.

Tensile stress may be increased until the reach of tensile strength, namely the limit state of stress.The formula for computing the tensile stress in a rod is:

$$\sigma = P / A \qquad (3.1)$$

where σ is the tensile stress, P is the tensile force over the rod and A is the cross-sectional area of the rod. Units for tensile stress are newtons per square meter (N/m^2, also called pascals, Pa)

3.4 POISSON'S RATIO

When a sample of material is stretched in one direction, it tends to get thinner in the other two directions. **Poisson's ratio** (ν, μ), named after Simeon Poisson, is a measure of this tendency. Poisson's ratio is the ratio of the relative contraction strain, or transverse strain (normal to the applied load), divided by the relative extension strain (in the direction of the applied load). For a perfectly incompressible material, the Poisson's ratio would be exactly 0.5.

3.5 SHEAR STRESS

In physics, shear stress is a stress state in which the shape of a material tends to change (usually by "sliding" forces) without particular volume change. The shape change is evaluated by measuring the relative change in the angle between initially perpendicular sides of a differential element of material (shear strain). A simple definition of shear stress is the components of stress at a point that act parallel to the plane in which they lie.

3.6 TENSILE STRENGTH

Tensile strength measures the force required to pull something such as rope, wire, or a structural beam to the point where it breaks.

Specifically, the tensile strength of a material is the maximum amount of tensile stress that it can be subjected to before failure. The definition of failure can vary according to material type and design methodology.
This is an important concept in engineering, especially in the fields of material science, mechanical engineering and structural engineering [3]: **Case, John, Lord Chilver, Carl T.F. Ross**, 1993.

There are three typical definitions of tensile strength:

1. Yield strength - The stress a material can withstand without permanent deformation.
2. Ultimate strength - The maximum stress a material can withstand.
3. Breaking strength - The stress coordinate on the stress-strain curve at the point of rupture.

3.7 YIELD STRENGTH

Yield strength or the yield point, is defined in engineering and materials science as the stress at which a material begins to plastically deform. Prior to the yield point the material will deform elastically and will return to its original shape when the applied stress is removed. Once the yield point is passed some fraction of the deformation will be permanent and non-reversible. Knowledge of the yield point is vital when designing a component since it generally represents an upper limit to the load that can be applied. It is also important for the control of many materials production techniques such as forging, rolling, or pressing.

In structural engineering, yield is the permanent plastic deformation of a structural member under stress. This is a soft failure mode which does not normally cause catastrophic failure unless it accelerates buckling.

3.8 PLASTIC DEFORMATION

In engineering mechanics, deformation is a change in shape due to an applied force. This can be a result of tensile (pulling) forces, compressive (pushing) forces, shear, bending or torsion (twisting) [4]: **Bijen, Jan,** 2003.

As seen at the Figure 3.1 next page, after reaching the plastic region, there is no turning back, where the deformation on the material is permanent and the standing force is also leading to a fracture.

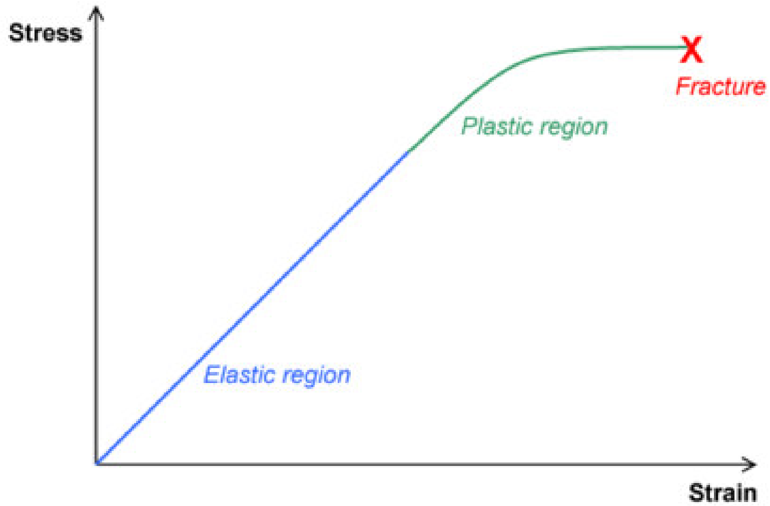

Figure 3.1: Diagram of a Stress-strain curve, showing the relationship between stress (force applied) and strain (deformation) of a ductile metal.

3.9 DUCTILITY

Ductility is the physical property of being capable of sustaining large plastic deformations without fracture (in metals, such as being drawn into a wire). It is characterized by the material flowing under shear stress.

3.10 DUCTILE MATERIAL

A ductile material is any material that yields under shear stress (as opposed to brittle fracture, which yields under normal stress). Gold, copper, and aluminium are highly ductile metals.

3.11 STRESS – STRAIN CURVE

A stress-strain curve is a graph derived from measuring load (stress - σ) versus extension (strain - ε) for a sample of a material (See Fig.3.2 and 3.3). The nature of the curve varies from material to material. The following diagrams illustrate the stress-strain behaviour of typical materials in terms of the engineering stress and engineering strain where the stress and strain are calculated based on the original dimensions of the sample and not the instantaneous values. In each case the samples are loaded in tension although in many cases similar behaviour is observed in compression [5]: **Budynas, Richard G. (Richard Gordon),** 1999.

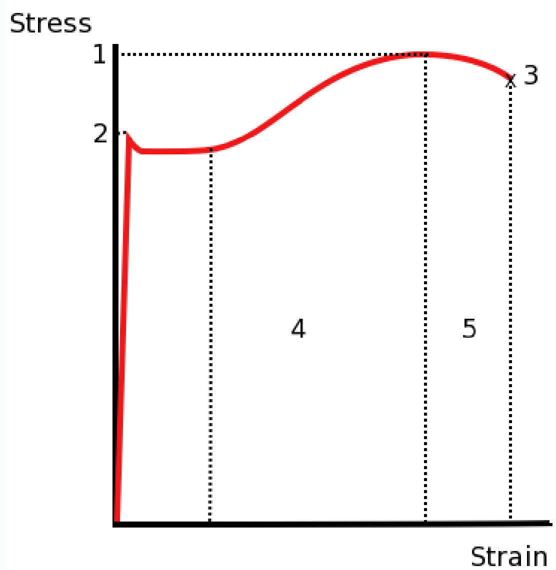

Figure 3.2: A stress-strain curve typical of structural steel
1. Ultimate Strength 2. Yield Strength 3. Rupture 4. Strain hardening region
5. Necking region.

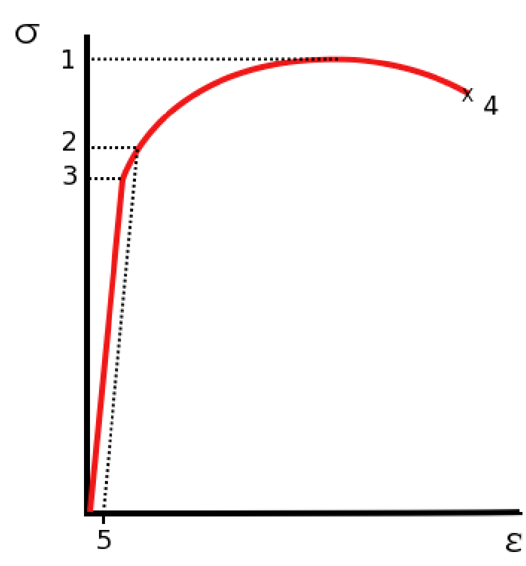

Figure 3.3: A stress-strain curve typical of aluminum
1. Ultimate Strength 2. Yield Strength 3. Proportional Limit Stress 4. Rupture
5. Offset Strain (typically 0.2%).

3.12 STRAIN HARDENING

Work hardening, or strain hardening, is an increase in mechanical strength due to plastic deformation. In metallic solids, permanent change of shape is usually carried out on a microscopic scale by defects called dislocations which are created by stress and rearrange the material by moving through it.

Plastic deformation induces a residual compressive stress in a peened surface, along with tensile stress in the interior.

3.13 RESIDUAL STRESS

Residual stresses are stresses that remain after the original cause of the stresses (external forces, heat gradient) has been removed. Residual stresses occur for a variety of reasons, including inelastic deformations and heat treatment. Heat from welding may cause localized expansion, which is taken up during welding by either the molten metal or the placement of parts being welded. When the finished weldment cools, some areas cool and contract more than others, leaving residual stresses. Castings may also have large residual stresses due to uneven cooling.

3.14 PRODUCTION METHODS for HARDENING

3.14.1 PEENING

Peening is the mechanical working of metals by means of hammer blows or by blasting with shot (shot peening). Peening is a cold work process. It tends to expand the surface of the cold metal, thereby relieving tensile stresses and/or inducing compressive stresses. Peening also encourages strain hardening of the surface metal.

3.14.2 SHOT PEENING

Shot peening is a process used to produce a decorative finish and to modify mechanical properties of metals. It entails impacting a surface with shot (round metallic particles) with force sufficient to create dimples and with enough shot that those dimples overlap. It is similar to sandblasting, except that it operates by the mechanism of plasticity (physics) rather than abrasion: each particle functions as a ball-peen hammer. In practice, this means that less material is removed by the process, and less dust created.

3.15 STIFFNESS

Stiffness is the resistance of an elastic body to deflection by an applied force. It is an intensive material property.

The stiffness k of a body that deflects a distance δ under an applied force P is:

$$k = P / б \quad (3.2)$$

Stiffness and is typically measured in newtons per metre.

As both the applied force and deflection are vectors (respectively P and δ), in general their relationship is characterised by a stiffness matrix, k where:

$$P = k\,\delta \quad (3.3)$$

The deflection can, in general, refer to a point distinct from that where the force is applied and a complicated structure will not deflect purely in the same direction as an applied force. The stiffness matrix enables such systems to be characterised in straightforward terms.

3.16 The S-N CURVE

In high-cycle fatigue situations, materials performance is commonly characterised by an **S-N curve**, also known as a **Wöhler curve**. This is a graph of the magnitude of a cyclical stress (S) against the cycles to failure (N).

S-N curves are derived from tests on samples of the material to be characterised (often called coupons) where a regular sinusoidal stress is applied by a testing machine which also counts the number of cycles to failure. This process is sometimes known as coupon testing. As an example, S-N Curve of

BrittleAluminium320 has been showed at the next page. (See Fig.3.4) There are also different kind of curves used by evaluation of the fatigue experiment results, which refer to the other approximation methods.

3.17 FINITE ELEMENT ANALYSIS

Visualization of how a car deforms in an asymmetrical crash using finite element analysis. Finite Element Analysis (FEA) is a computer simulation technique used in engineering analysis. It uses a numerical technique called the finite element method (FEM).

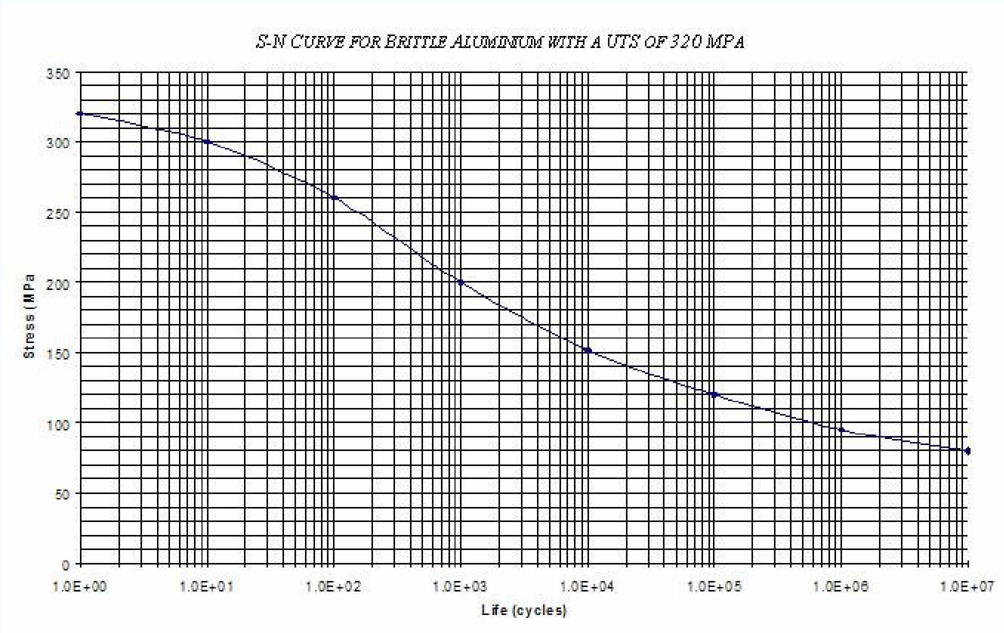

Figure 3.4: S-N Curve of Brittle Aluminium of 320 MPA

Development of the finite element method in structural mechanics is usually based on an energy principle such as the virtual work principle or the minimum total potential energy principle. While being an approximate method, the accuracy of the FEA method can be improved by refining the mesh in the model using more elements and nodes.

A common use of FEA is for the determination of stresses and displacements in mechanical objects and systems.

3.18 ANSYS SOFTWARE

ANSYS is the original general-purpose finite element analysis software and is a general purpose finite element modeling package for numerically solving a wide variety of mechanical problems.

ANSYS software is also used to analyze different kind of problems in the area of Civil Engineering, Electrical Engineering, Physics and Chemistry.

3.19 CAR SUSPENSIONS

All of the power generated by a piston engine is useless if the driver can't control the car. That's why the suspension system is very important for the engineers by the design of an automobile as much as the four-stroke internal combustion engine.

Figure 3.5: Car Suspension drawings from different views (3D models are downloaded from the web site : www.turbosquid.com).

The job of a car suspension (See Fig.3.5) is to maximize the friction between the tires and the road surface, to provide steering stability with good handling and to ensure the comfort of the passengers.

If a road were perfectly flat, with no irregularities, suspensions wouldn't be necessary. But even freshly paved highways have imperfections that can interact with the wheels of a car. It's these imperfections that apply forces to the wheels. According to Newton's laws of motion, all forces have both magnitude and direction. A bump in the road causes the wheel to move up and down perpendicular to the road surface. The magnitude, of course, depends on whether the wheel is striking a giant bump or a tiny speck. Either way, the car wheel experiences a vertical acceleration as it passes over an imperfection (See Fig.3.6).

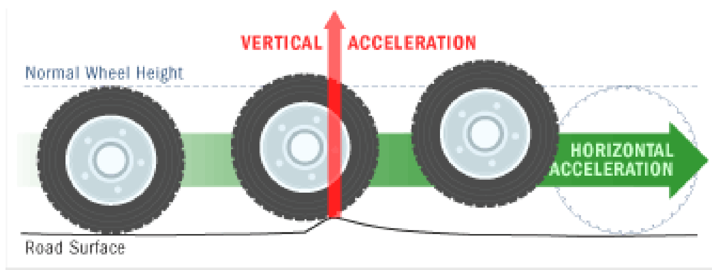

Figure 3.6: Vertical/Horizontal Acceleration

Without a structure between, all of wheel's vertical energy is transferred to the frame, which moves in the same direction. In such a situation, the wheels can lose contact with the road completely. Then, under the downward force of gravity, the wheels can slam back into the road surface. Under these circumstances is a system needed that will absorb the energy of the vertically accelerated wheel, allowing the frame and body to ride undisturbed while the wheels follow bumps in the road.

3.20 The Chassis

The suspension of a car is actually part of the chassis, which comprises all of the important systems located beneath the car's body (See Fig.3.7).

Figure 3.7: Chassis Drawings (3D models are downloaded from the web site : www.turbosquid.com).

These systems include:

- The frame - structural, load-carrying component that supports the car's engine and body, which are in turn supported by the suspension
- The suspension system - setup that supports weight, absorbs and dampens shock and helps maintain tire contact
- The steering system - mechanism that enables the driver to guide and direct the vehicle
- The tires and wheels - components that make vehicle motion possible by way of grip and/or friction with the road

So the suspension is just one of the major systems in any vehicle [1]: **Hurd, N.J.,** 1996.

4 EXPERIMENTAL METHODS

Figure 4.1: Stabilizer bar supported at one end and forced at the other one.

4.1 HYDROPULS TEST STAND and SERIES 244 ACTUATORS

Fatigue Tests are carried out through a specific mechanism called "Hydropuls Test Stand" which has an independent ground of the workstation surface, so that it is isolated from outer vibration sources. That unique table ensures a safe area to make fatigue and strength researches by retaining the necessary equipment on itself [a,*]. There are hydraulic pumps and fittings needed in order to carry out high cycled fatigue tests and this time Series 244 Hydraulic Actuators [b,*] are used to provide an integrated, high performance solution to dynamic force requirements [13]: **mts.com**.

---

a. See Figure 4.1 for test mechanism
b. See Figure 4.2 for the Series 244 Hydraulic Actuator

Each of the actuator components and options helps simplify the process of designing and building high performance testing systems. Actuators are used in demanding vehicle dynamics, structural fatigue and component test applications.

Actuators are manufactured for years of reliable operation in servohydraulic test systems. Series 244 Hydraulic Actuators are optimized to provide the components and capabilities required by dynamic testing applications.

Figure 4.2: Series 244 Hydraulic Actuators

4.2 FEATURES OF SERIES 244 ACTUATORS

These Actuators demonsrate superior reliability and versatility in force ratings from 15 to 1000 kN. The standard stroke lengths for the Series 244 Hydraulic Actuators are 152.4 and 254.0 mm with approximately 25.4 mm of piston rod jumping from the front end when fully retracted. These specifications can be altered to adapt the actuator to a variety of testing requirements and configurations.

Standard Series 244 HydraulicActuators accept servovalves with flow ratings up to 340 L/min. Optional porting can be provided to increase the flow requirements.

4.2.1 SPECIFICATIONS

The specifications for the Series 244 Hydraulic Actuator models are shown on the following table.

Table 4.1: Specifications for Basic Cylinder Size and Mounting
– related with Fig.4.3 -

Model	Force Rating [kN]	Rod Diameter [mm]	Piston Area [cm2]	Cushions (A) [mm]
244.20	68	69,9	33,68	10,2

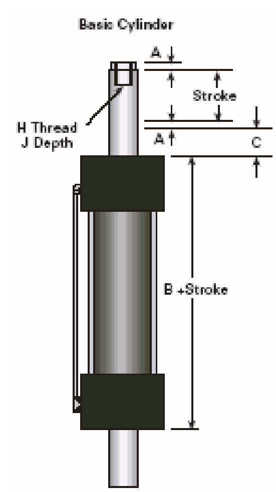

Figure 4.3: Basic Cylinder

Figure 4.4: Stabilizer is also fixed around the both bearings along its axis.

As on the Figure 4.4, it is clearly seen that the fixtures are demonstrating the bearings where the rod is suited on the vehicles chassis. The Stabilizer Bar actually is assembled on the both ends of the axle, because the rotating motion on itself must be prevented through bearings in order to optimize its duty of mechanical absorption.

4.3 TEST METHODS

Correlating metals fatigue and fracture to materials properties requires extensive analysis and testing. The control of fracture and fatigue has become a high priority of designers and materials researchers [9]: **Tada, Hiroshi, Hiroshi Tada, Paul C. Paris, George R. Irwin,** 2000.

Key factors in performing fatigue tests are:

1. Specimen alignment
2. Specimen surface condition
3. Precision in setting and maintaining cyclic loading parameters and test frequency

Such tests are useful in developing data from mechanical design, materials, process and quality control, product performance and failure analysis.

Much valuable information can be obtained regarding the stability of materials under cyclic loading or whether changes occur due to cyclic plastic straining and when crack begin to from.

In other words, fatigue tests are made with the object of determining the relationship between the stress range and the number of times it can be applied before causing failure. Testing machines are used for applying cyclically varying stresses and cover tension, compression, torsion and bending or a combination of theses stresses.

At this work Stabilizer bars are examined as specimen in order to determine a substitute supplier and optimize the strength characteristic of the part. The Stress Strain relation of different specimens are observed and measured.

Strain is defined as the amount of deformation per unit length of an object when a load is applied (a,*). Strain may be compressive or tensile and is typically measured by strain gages. Fundamentally, all strain gages are designed to convert mechanical motion into an electronic signal. A change in capacitance, inductance, or resistance is proportional to the strain experienced by the sensor called strain gage (See Fig.4.5).

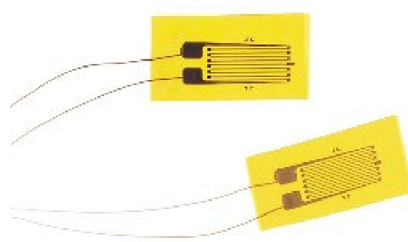

Figure 4.5: The most universal measuring device for the electrical measurement of mechanical quantities is the strain gage. Several types of strain gages depend on the proportional variance of electrical resistance to strain.

a. See Part 3 : Theoretical Methods

5 TECHNICAL EXAMINATION - DIFFERENT SUPPLIERS SPECIMEN

5.1 GENERAL PROCEDURE

To increase the durability of the stabilizer, samples from three different suppliers [a,*] are tested with respect to Wöhler [b,*] criteria. Company A as the main supplier has also applied shot peening [c,*] process to the samples and has bought a new CNC tube bending maschine in order to produce stabilizers of better quality by improving the mechanical properities.

By the way the difference between the Company B samples is that the second type of samples are produced with serial fixture and shot peening, because of the unsuccessfully test results of the prototype.

Company C has offered a new design of stabilizer rod, which was not proper for the vehicles suspension mechanism itself, but got remarkably good solutions at tests.

Obtained results are comparatively depicted on an S-N curve to determine the durability. The chemical properties of materials were another criteria, however the specimens produced with new materials and their additives picked up the level of durability also higher.

---

a. Because of the "Corporate Identity" issues, the names of suppliers are mentioned as Company A, Company B and Company C
b. See: Theoretical Methods, Wöhler Curves
c. See: Theoretical Methods, Shot-peening

5.2 EXPERIMENT I - PROCEDURE

The tests aim to compare the fatigue life characteristics of the stabilizers of Co.A with its substitutes of Co.B. The models are forced under the same testing conditions and the resulting Wöhler curves are constructed. As in the fatigue tests, the comparison criteria is these Wöhler curves. According to these characteristic curves, the difference between the fatigue lives of the both types will be deduced [8]: **Piper, D. E,** 1970.

The tests will be carried out for both front and rear axles and the considered stabilizers are; front axle (see Fig.5.1) and rear axle (see Fig.5.2).

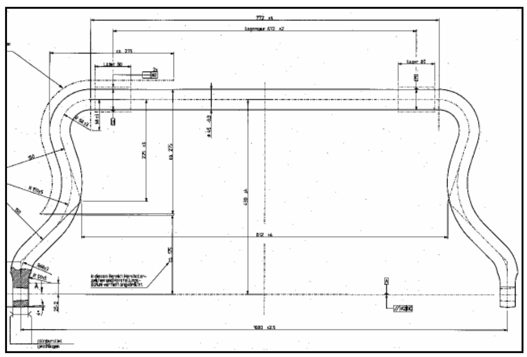

Figure 5.1: The front axle stabilizer

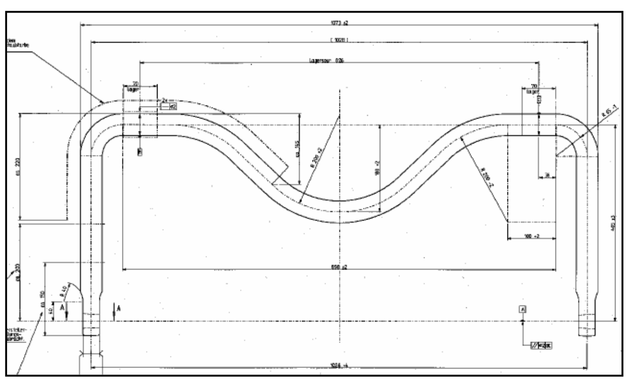

Figure 5.2: The rear axle stabilizer

5.3 TEST RESULTS

The results of the comparatively conducted fatigue tests between Co.A and Co.B stabilizers have showed that the fatigue life of the Co.B stabilizers is less than the Co.A stabilizers. Namely, the fatigue life of the Co.B stabilizers is approximately 20-22% lower than the serially used ones. Sharing this information with the supplier revealed that the samples are just on prototyping stage and there would be differences between the serially produced samples and the prototypes. The tests will be continued with the samples produced by the serial fixture.

As a requirement of redesign, geometrical conformity of the samples to the technical drawings must be ensured. After that, new samples manufactured using serial production fixtures are required to continue the tests.

5.3.1 TEST PHASE

For conducting the tests of stabilizers, the setup [a,*] shown in Figure 5.3 is used.

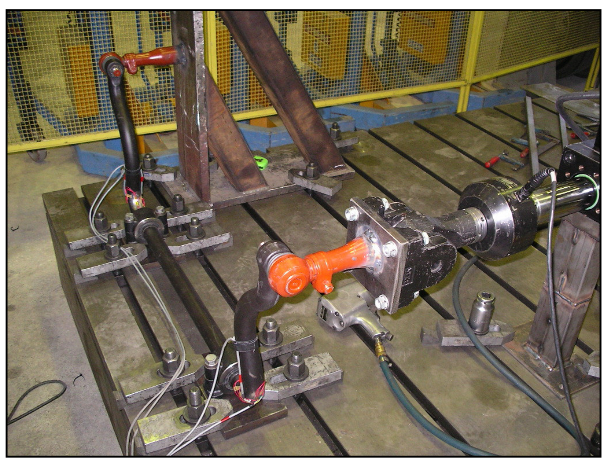

Figure 5.3: Test setup

---

a. For detailed information about the so called "Hydropuls test stand", See: Experimental methods

Tests are performed one-dimensional and in each loading level more than one specimen are tested for both Co.A and Co.B stabilizers. Before going into the tests, FEM [a,*] calculations have been performed with the same boundary conditions and the critical areas are figured in Figure 5.4.

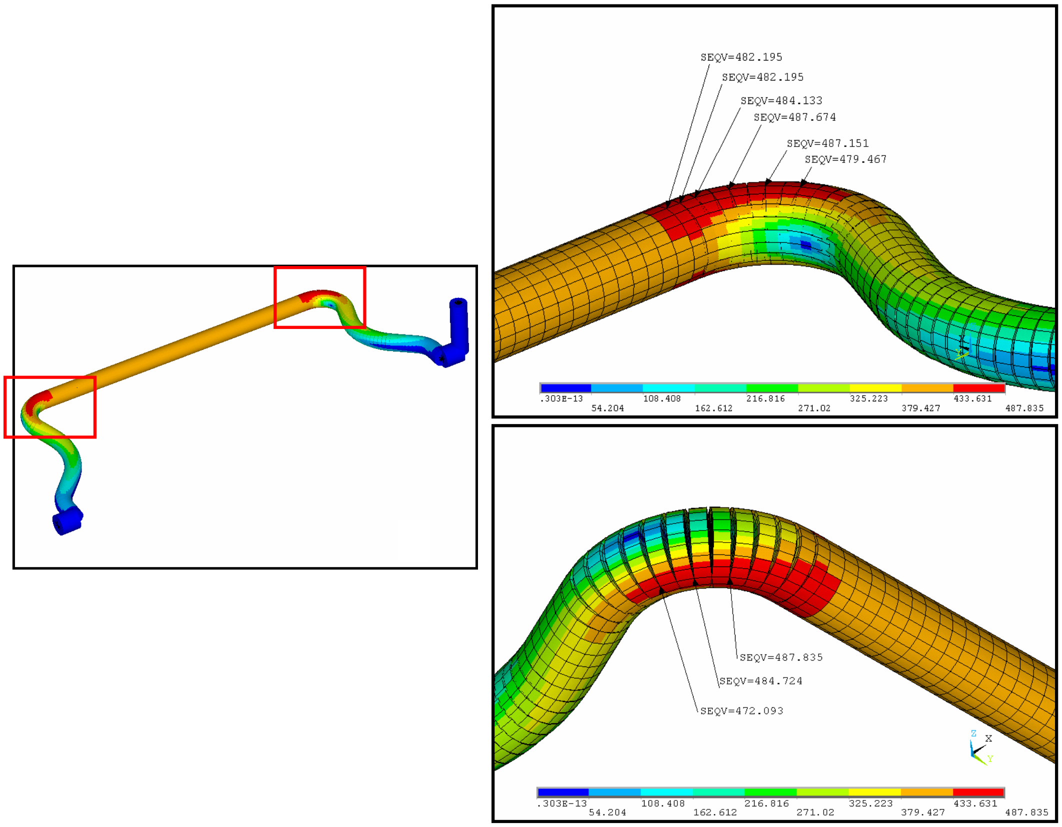

Figure 5.4: FEA results

The succeeded test results are listed in Table A.1 [b,*]. In this table the tests that are finished up to now are listed.

---

a. FEM is a mathematical approximation method for durability analysis. For further tech.info. about ANSYS software and FEM, see: Experimental methods - Part 4.
b. For Table A.1, see Appendix A

The Figures 5.5 through 5.8 show both the fracture points of the samples and the samples after the tests. As seen in the figures, there is a confirmation between the results of the tests and FEA.

Meshed surfaces painted in different colors present critical parts of the beam with a simple principle. The level of durability has been showed via a light spectrum, where the colors of the parts under extremely high pressure differ in color. Locations carrying much higher stress then the rest of the beam turn into red. While stress-strain values are decreasing, the color tends to turn into the blue.

The fracture points of both Co.A and Co.B stabilizers show similarity, they are broken from the most expected sections. To see whether the performance difference still exists for the rear axle stabilizers, one sample from each type is tested.

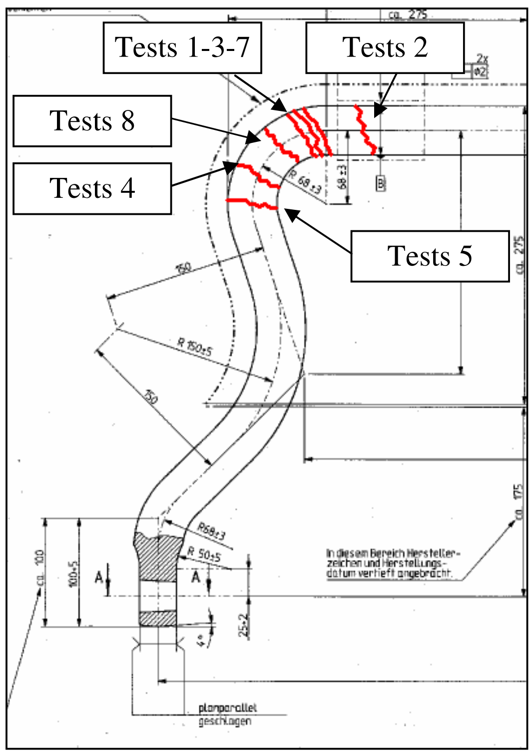

Figure 5.5: Fracture points for the serial stabilizers

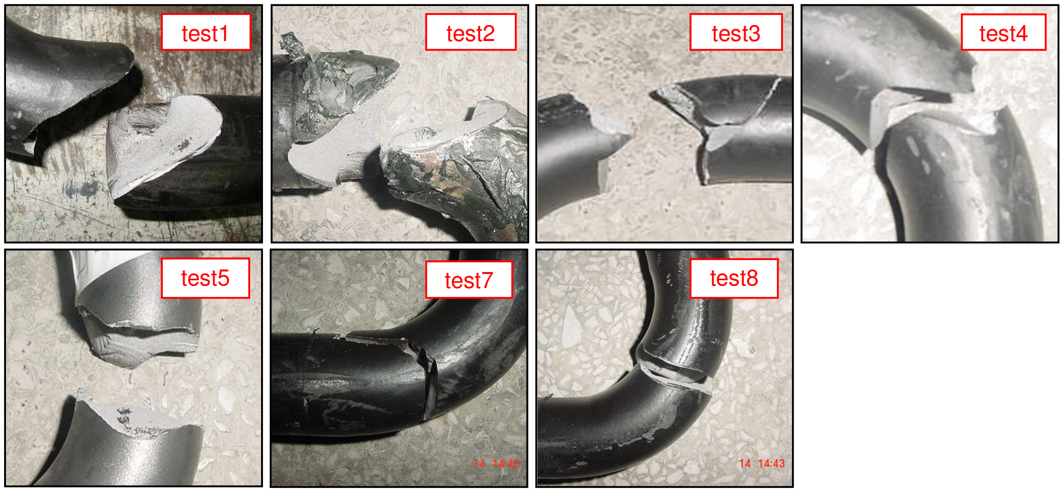

Figure 5.6: Fractured serial stabilizers

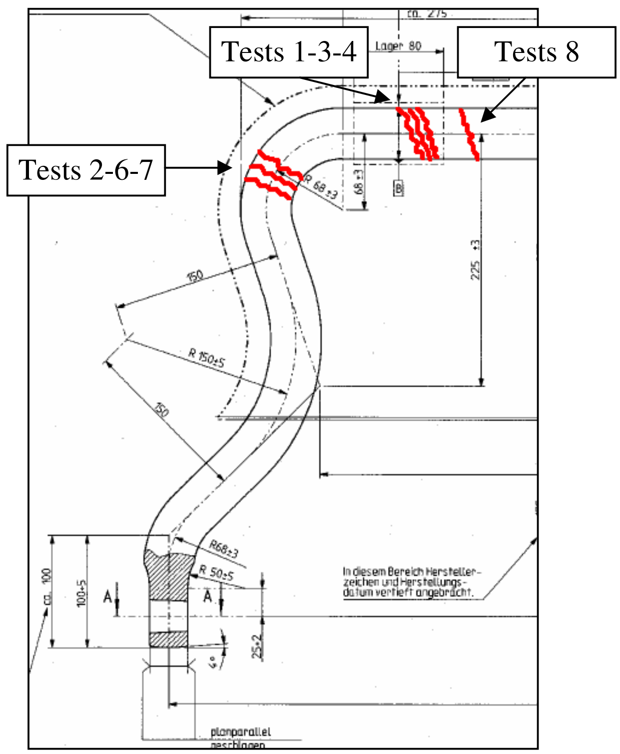

Figure 5.7: Fracture points for Co.B stabilizers.

Figure 5.8: Fractured Co.B stabilizers

After the obtained results, the Wöhler curves, see Figure 5.9 and 5.10 are constructed for both Co.A and Co.B stabilizers. These curves are drawn according to the points of fracture. In Figure 5.9, the results of the tests are put together into a typical Wöhler curve. This figure shows the general characteristics of the material 50CrV4 [a,*]. From this figure, it is also clear that the stabilizers of the Co.B lie mostly in lower scattering range and the Co.A stabilizers in the upper scattering range of the Wöhler curve.

Also the scatter on the fracture cycles with the same force values can be explained by the difference on the stiffness [b,*] of the specimens [11]: **A. Rinaldi, P. Peralta, D. Krajcinovic, Y.-C. Lai,** 2005. A separate view of the average value of the results on Figure 5.10 clarifies the life span difference, showing that the fatigue lives of the Co.B stabilizers is 20-22 % lower than that of Co.A Also tests of the rear axle stabilizers showed that the durability performance of Co.B is still lower than that of Co.A. But as declared before, the tests will be repeated with the samples produced by the serial fixture.

---

a. See: Appendix B for the Section Chemical Properties of Materials
b. See: Theoretical Methods, Stiffness of Materials

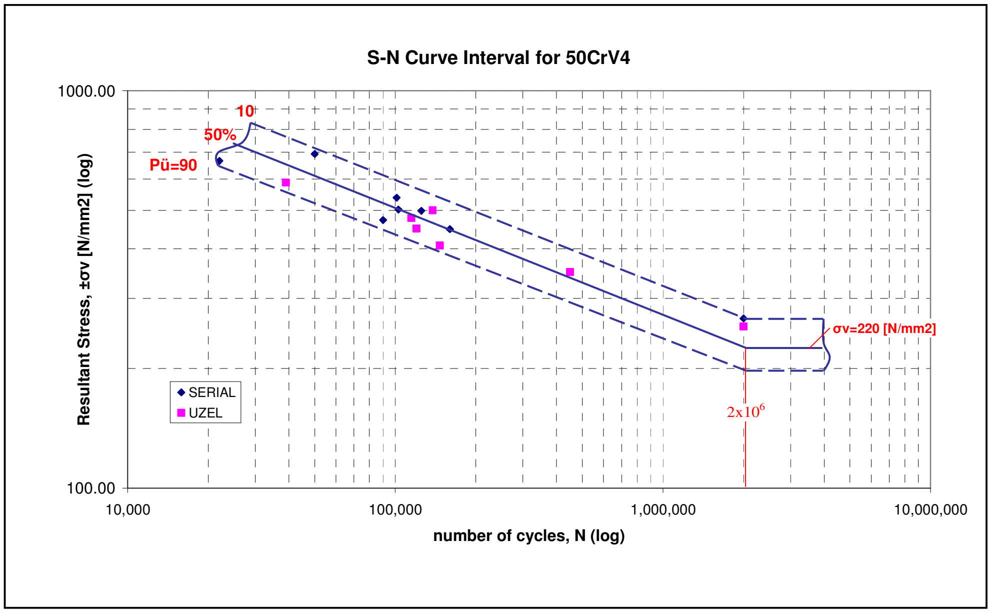

Figure 5.9: Complete S-N curve for 50CrV4.

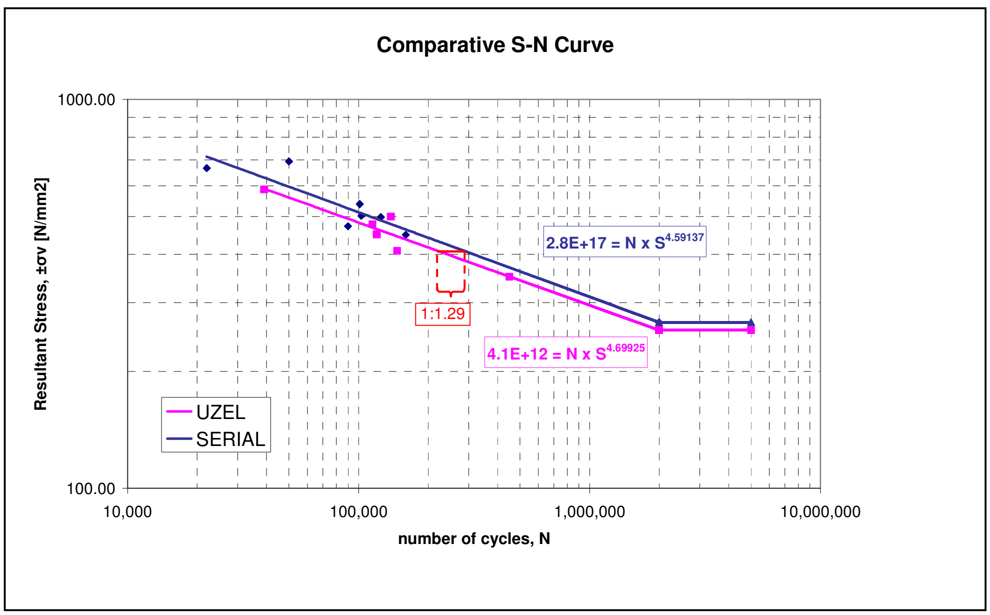

Figure 5.10: Comparative S-N Curves.

5.4 EXPERIMENT II - PROCEDURE

The tests aim to compare the fatigue life characteristics of the stabilizers of Co.A with its substitutes of Co.B and Co.C. The differences of the tests from the former test are that the samples of Co.A are shot-peened [a,*] and Co.B samples are manufactured with the serial fixture. The Co.C samples are adding a new approach with its new form. The samples are forced under the same testing conditions and the resulting Wöhler curves are constructed. The comparison criterion is these Wöhler curves. Throughout the tests, as in the former one, fatigue testing standard of DIN 50100 is followed.

The tests will be carried out for only front axle's stabilizers. The samples under examination are front axle of Co.A (see Fig.5.11) and front axle of Co.C (see Fig.5.12) as showed below.

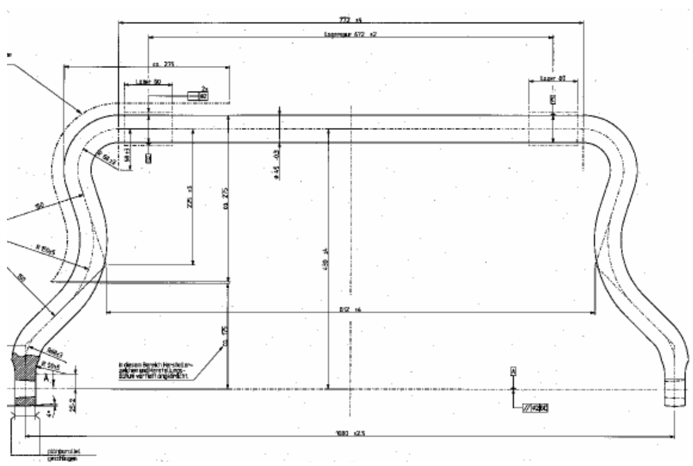

Figure 5.11: The front axle stabilizer of Co.A

---

a. See: Theoretical Methods, Shot-peening
b. DIN 50100 (stands for Deutsche Industrie Norm) defines the fatigue testing method, also called as "Continues Vibration Test"

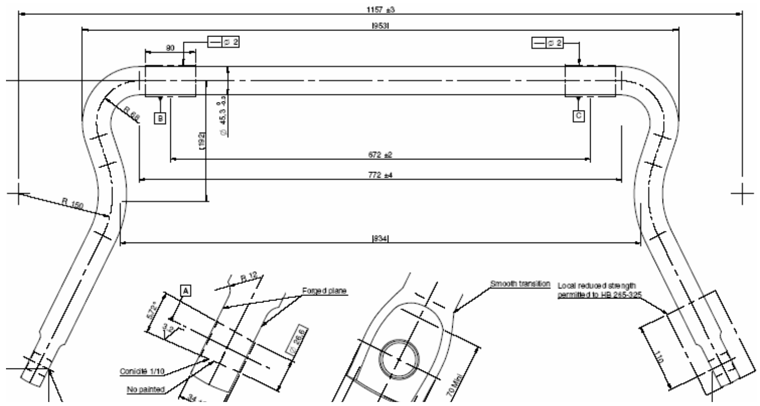

Figure 5.12: The front axle stabilizer of Co.C

5.4.1 TEST RESULT

Tests were conducted with the samples of Co.C, Co.A and Co.B. Table A.2 [a,*] figures out the results of the tests and Figure 5.13 and 5.14 depict the results comparatively. According to Figure 5.13 and 5.14 Co.C with its new form is the most durable stabilizer. It is almost triple times more durable than Co.A and Co.B. Co.A and Co.B have resulted on almost the same durability characteristics. Their Wöhler lines coincide with a difference of that below 10.33 kN Co.A is slightly more durable, below 10.33 kN Co.B is slightly more durable stabilizer. These ratio is more clearly seen on Figure 5.14, which is constructed to show the results of 10 and 11 kN comparatively.

To conclude, with respect to the durability point of view Co.C and Co.B can be considered as good substitutes for the serially used Co.A stabilizer.

As a requirement of redesign, applicability of the new geometrical form of Co.C and must be ensured. Manufacturing processes of the Co.B stabilizers must be improved.

a. For Table A.2, see Appendix A

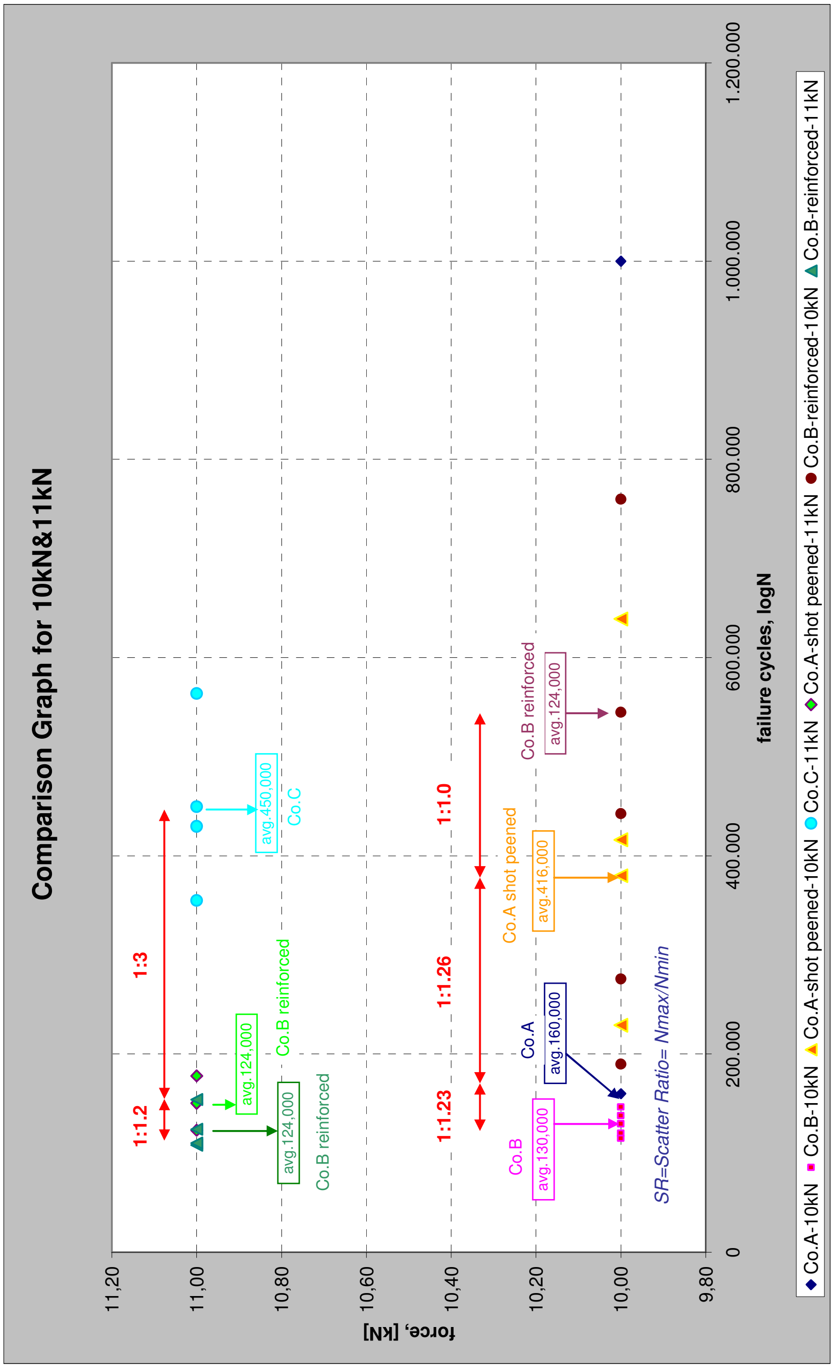

Figure 5.13: Comparison graph for 10 and 11 kN.

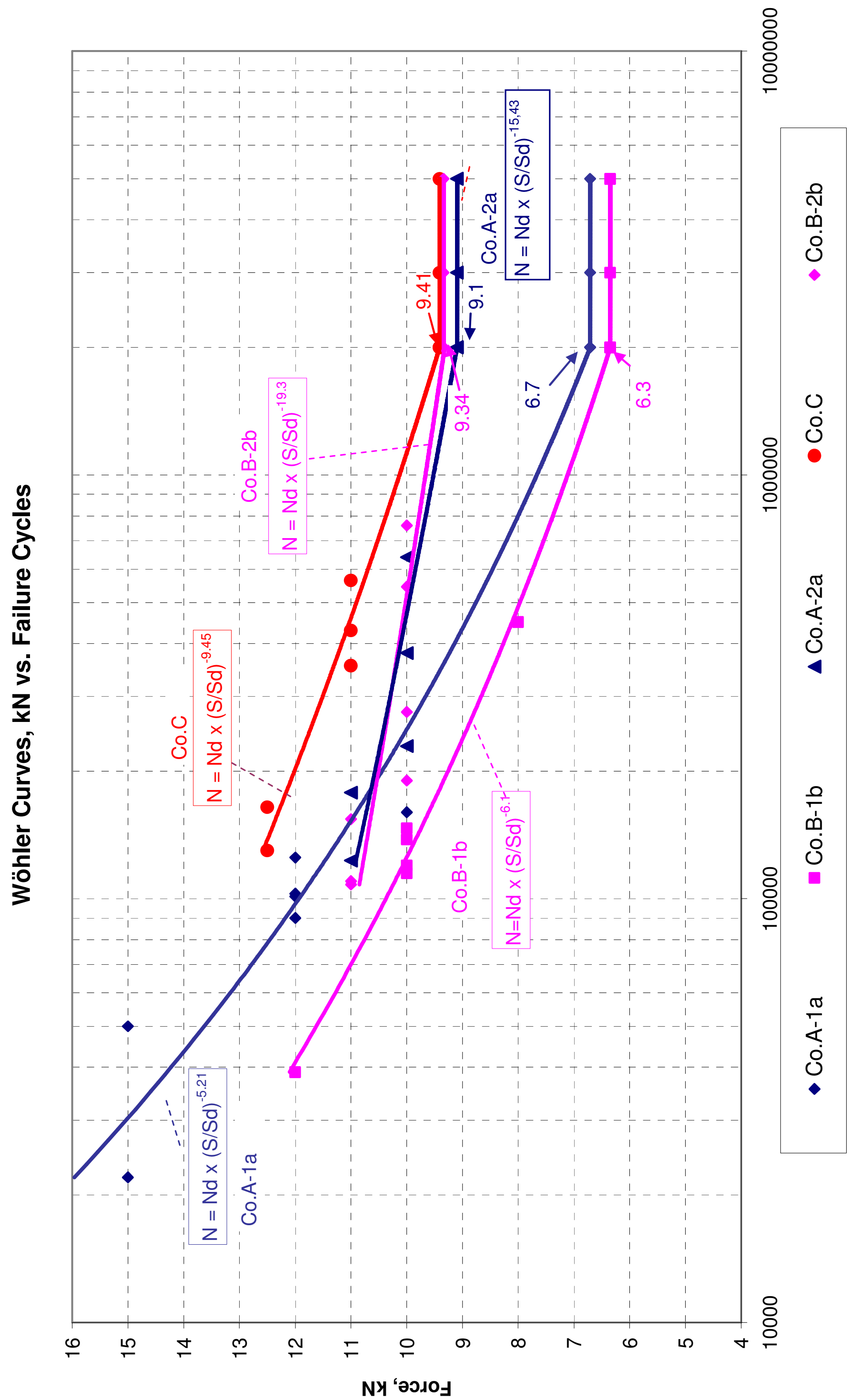

Figure 5.14: Wöhler Curves vs. Failure Cycles

The differences of the conducted tests from the former tests are only on the test samples. The setup, testing method and the evaluation criterion are all kept same. One of the samples, Co.A, has gone through the shot peening process, while Co.B samples are produced by using a serial fixture with again shot-peening process. As a third substitute, Co.C with its new form and new material is tested. Instead of 50CrV4, 61SiCr7 [a,*] is used on Co.C samples.

The succeeded test results are listed in Table A.2 [b,*]. After the obtained results, the Wöhler curves, see Figure 5.14, are constructed for all of the test samples. This figure also shows the before and after values of Co.A and Co.B. According to these values, the slope of the curves which is a description of material property has drastically increased in the new samples, from 5.21 to 15.43 for Co.A and from 6.1 to 19.3 for Co.B.

When the three samples are compared, Co.C has the highest strength and Co.A and Co.B samples come second with almost equal durability characteristics. Wöhler curves of these two samples coincide at 10.33 kN and above this value Co.A, below this value Co.B is slightly more durable.

Figure 5.13 is constructed for the purpose of comparison on kN-basis. This figure clearly shows that the applied processes increased the fatigue life of the samples drastically. Application of shot peening has increased the life of Co.A with a ratio of 1:2.6, while manufacturing by serial fixture instead of prototype fixture increased the life of Co.B by 1:3.4. It also shows that Co.C samples are almost triple times more durable

than the other samples. As another result, at 10 kN, Co.B-reinforced samples is slightly more durable, while at 11 kN Co.A samples are approximately 20 % more durable.

---

a. See: Appendix B for the Section “Chemical Properties of Materials”
b. For Table A.2, see Appendix A

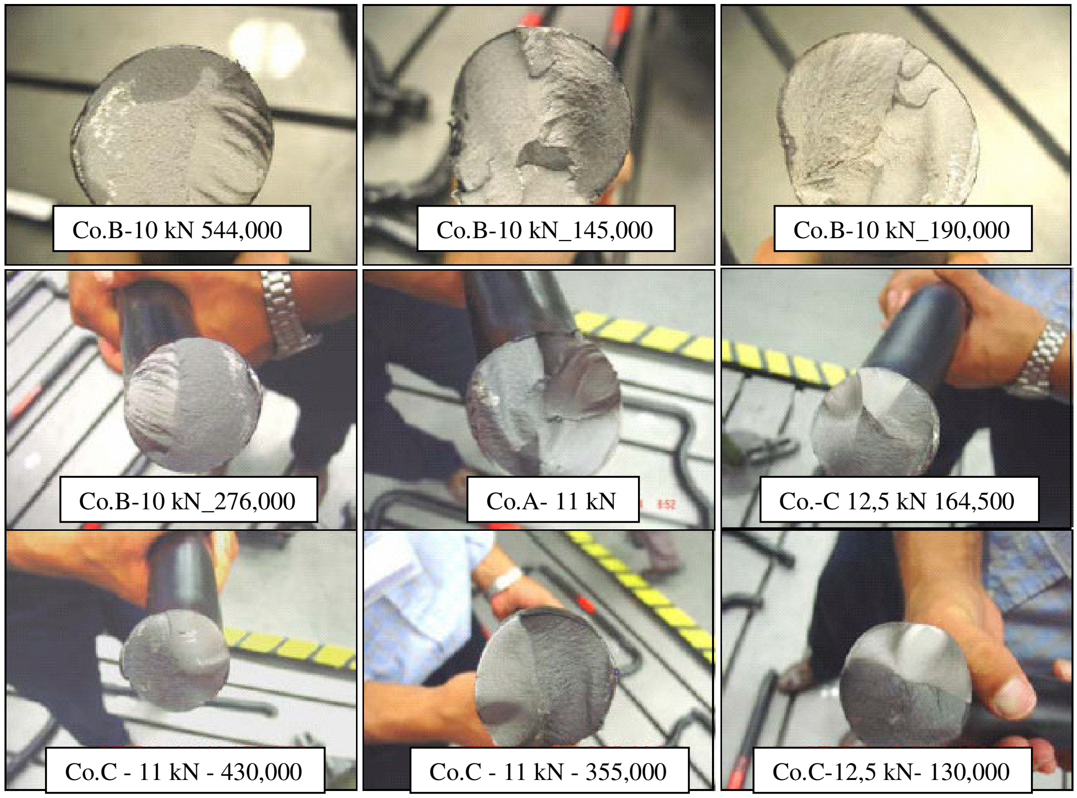

Figure 5.15: Several fractured samples

Throughout the tests, the objective was to apply the fatigue standards clearly. This effect, fatigue lines, can be clearly seen on the fractured surface of the samples, see Figure 5.15.

To summarize, Co.C with its new form and new material brings a high level standard with respect to the durability point of view. At the same time, it has been proved that new Co.B samples are a good substitute for the serially used Co.A samples. Also, the further developments will base on the material and the manufacturing processes.

5.5 EXPERIMENT III - PROCEDURE

The differences of the Co.B and Co.A samples from the former ones are that Co.B had proposed a new material, 51CrMoV4 [a,*], and Co.A had proposed both a new material and a new production process. The tests have been conducted according to the fatigue testing standard of DIN 50100.

Throughout the tests durability characteristics, scatter and the stiffness values of the samples are taken into account. The results of the tests are presented in comparative Wöhler curves together with the results of the former tests.

5.6 RESULT

As a continuation report, this study examines the fatigue life characteristics of Co.A and Co.B samples after several changes both in material and the production process and make comparisons between the all samples tested up to now. Test samples are evaluated with respect to durability characteristics, distribution of the failure cycles and the stiffness values.

Co.B with its new material, 51CrMoV4, had the highest durability after the tests, as shown on Figure 5.14. It is 2 times more durable than Co.C samples and at least 6 times more durable than the other samples. Both the scatter characteristics and the stiffness values show quite acceptable values. In spite of the best scatter characteristics, Co.A samples that are produced from automatic bending machine results on the unsatisfactory durability characteristics.

To conclude, when the durability results are analyzed thoroughly together with the results of the earlier tests, Co.B-51CrMoV4 is the best substitute for the serial production and can be released with respect to durability point of view.

---

a. See: Appendix B for the Section Chemical Properties of Materials

5.7 EXECUTION

As it is already known, to test and conclude about the durability characteristics of front axle's stabilizer bar, 3 different groups of samples were delivered up to now. The history of these tests is summarized in Table 5.1. Notation of this table will be used throughout the report.

Table 5.1: History of the Tests

Group	Supplier	Material	Production Process	Results
1	Co.A	50CrV4	serial	low durability
	Co.B	50CrV4	prototype fixture	low durability
2	Co.A	50CrV4	shot peening	higher durability, high scatter
	Co.B	50CrV4	serial fixture	higher durability, high scatter
	Co.C	61SiCr7	with new geometrical form	high durability
3	Co.B	51CrMoV4	serial revised fixture	highest results, low scatter
	Co.B	50CrV4+	with Boron additives	tested by Co.B itself
	Co.A	50CrV4	automatic bending maschine	low durability, lowest scatter
	Co.A	61SiCr7	automatic bending maschine	lowest durability

The final group consists of samples with different material and different production techniques. Co.A has delivered two different stabilizer bars, one is produced from 50CrV4, and the other is produced from 61SiCr7. And also, as a new production technique, both of the samples are produced from a new automatic bending machine. However Co.B has delivered 2 different samples, one is made of 51CrMoV4 and the other is made of 50CrV4 with Boron additives. Except Co.B-50CrV4 with Boron, all samples were tested at the last experiment.

Test samples are also investigated with respect to their geometry and the chemical compositions. Table 5.2 summarizes the chemical compositions of the materials used in the testing samples. It is a well known fact that both molybdenum and chromium compositions increase the toughness of the material and impart hardenability and resistance to softening. The geometrical measurement of the specimen is made through a 3D coordinates measuring machine and the results have showed no critical values out of tolerances.

Table 5.2: Chemical compositions of the materials

Chemical Analysis								
Material	Composition (wt %)							
	C	Mn	Si	P	S	Cr	Mo	V
50CrV4	0,47	0,5	0,4	0,025	0,025	0,8		0,1
	0,55	0,8	max	max	max	1,2		0,25
61SiCr7	0,57	0,7	1,6	0,025	0,025	0,9	0,15	0,1
	0,65	1	2	max	max	0,45		
51CrMoV4	0,48	0,7	0,4	0,025	0,025	0,9	0,15	0,1
	0,56	1,1	max	max	max	1,2	0,3	0,2

The scatter of the failure cycles is also an evaluation criterion. To compare the scatter characteristics of the samples a scatter ratio has been defined which is the ratio of maximum failure cycle to minimum failure cycle, SR=Nmax/Nmin. Although scatter ratio changes according to the load level but modern durability analysis requires a scatter ratio of around 3. Therefore, how far the scatter ratio below 3 is, more repeatable and more acceptable the test results are.

5.8 SINGLE RESULT

The setup, testing method and the evaluation criterion are kept same as in the former tests.The obtained test results are evaluated with respect to the durability, scatter and stiffness point of views, see Tables A.3 and A.4 [(a,*)]. The results are depicted on the related figures comparatively with the results of the earlier tests. For different materials Wöhler lines have different slopes. Therefore comparisons are done for each load levels separately as seen on Figures 5.16 and 5.18.

a. For Table A.3 and A.4, see Appendix A

5.9 RESULTS of CO.B SPECIMEN

At 10 kN, see Figure 1, durability of first and second groups of Co.B samples (according to their averaged values) has a ratio of 1:2.52. However the graph does not include Co.B-3a samples, since failure cycles of these go beyond 1,000,000 cycles, which is the stopping criteria. In Figure 5.17 a better comparison between three different Co.B samples can be done under 11 kN. Co.B-3a with a single value of 885,000 shows a noticeable result which is almost 7-fold more durable than Co.B-2b. Scatter characteristics of Co.B can be seen comparatively on Figures 5.17 and 5.18. While it is 4 in the second group, it decreases to 1.61 in the last samples.

When Figure 36 is analyzed, following values are obtained for the Co.B samples;

Table 5.3: Comparison of samples

Knee point (kN)		Slope
Co.B-1b →	6,3	-6,1
Co.B-2b →	9,34	-19,3
Co.B-3a →	10,75	-14,51

Those show that Co.B-3a samples have the uppermost Wöhler line.

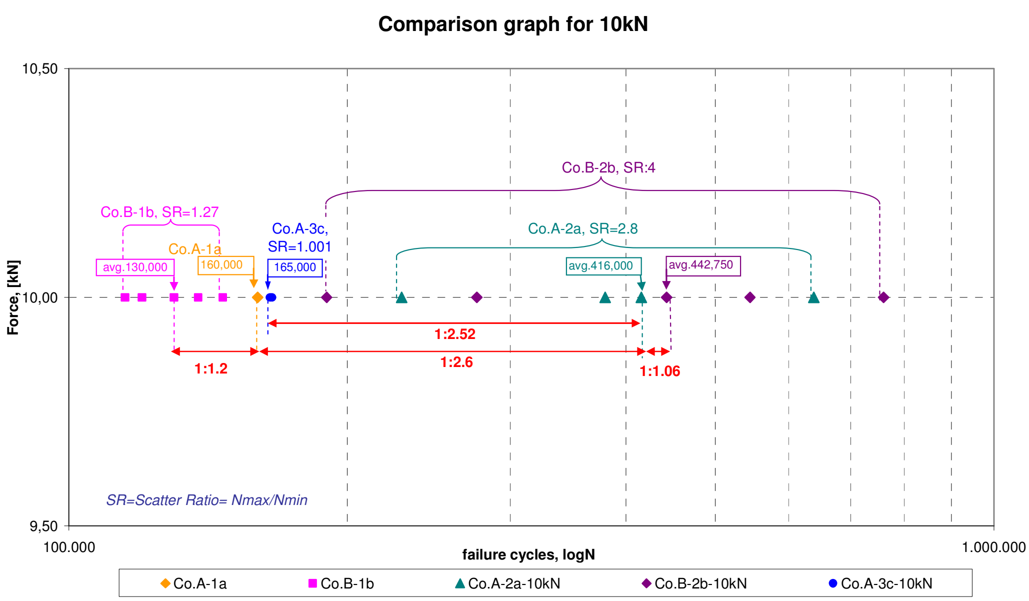

Figure 5.16: Comparative graph for 10kN.

5.10 RESULTS of CO.C SPECIMEN

Co.C offers a new geometrical form with 61SiCr7 material. Among the others Co.C has the heaviest weight with 23,34 kg. Figure 40 shows that Co.C samples have an averaged failure cycle of 450,000 under 11 kN, which is three times more durable than Co.A

samples. But when Figure 40 and 41 are examined comparatively, it is seen that Co.C samples are approx. 60% less durable than Co.B-3a samples.

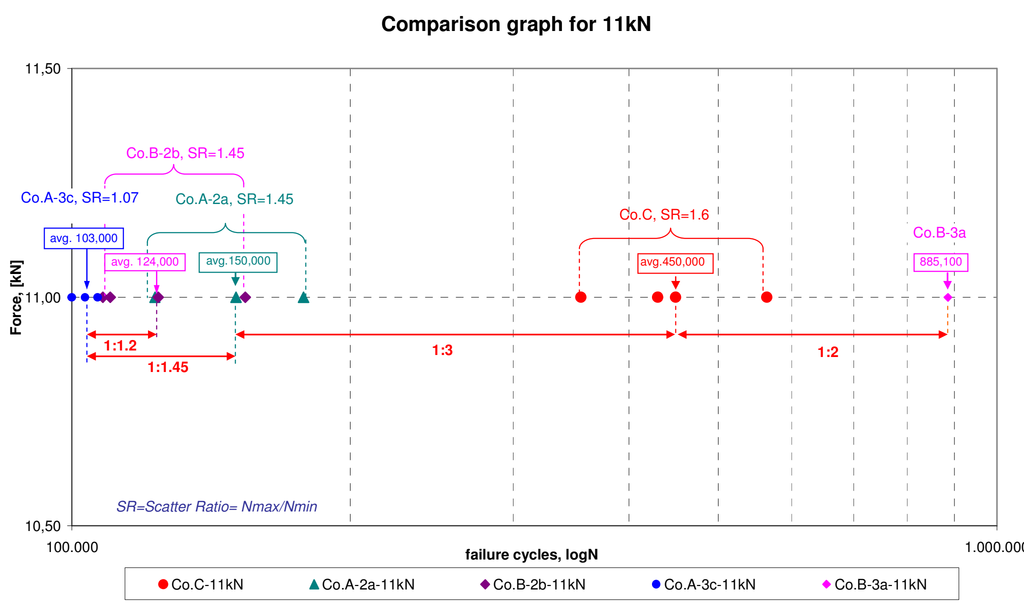

Figure 5.17: Comparative graph for 11kN.

Scattering characteristics of Co.C is quite acceptable with an averaged value of 1,43. Figure 36 gives the Wöhler line of Co.C samples as

$N = N_d \times (S/S_d)^{-9.45}$ where S_d=9.41 at N_d=2,000,000

5.11 RESULTS of CO.C SPECIMEN

Last group of Co.A differ from the previous serial and shot peened types with respect to material and productions techniques. The samples that are made of 50CrV4 and 61SiCr7 are produced from an automatic bending machine.

However this last group with 50CrV4 does not show good results with respect to the durability point of view. At 10 kN, Figure 39, the averaged failure cycles of Co.A-1a,

-2a, -3c are 160.000, 416.000 and 165.000 respectively which shows a worse durability for Co.A-3c in spite of a better scattering characteristics (from 2,8 to almost 1). Figure 40 shows almost the same characteristics; failure cycles of 150,000 and 103,000 for Co.A-2a and Co.A-3c respectively. Figure 43 gives the Wöhler line of Co.A-50CrV4 as;

$$N = N_d \times (S/S_d)^{-11.3} \text{ where } S_d\text{=8.26 at } N_d\text{=2,000,000}$$

The case with 61SiCr7 is the worst one. The results stay at the lowest position with the lowest Wöhler line.

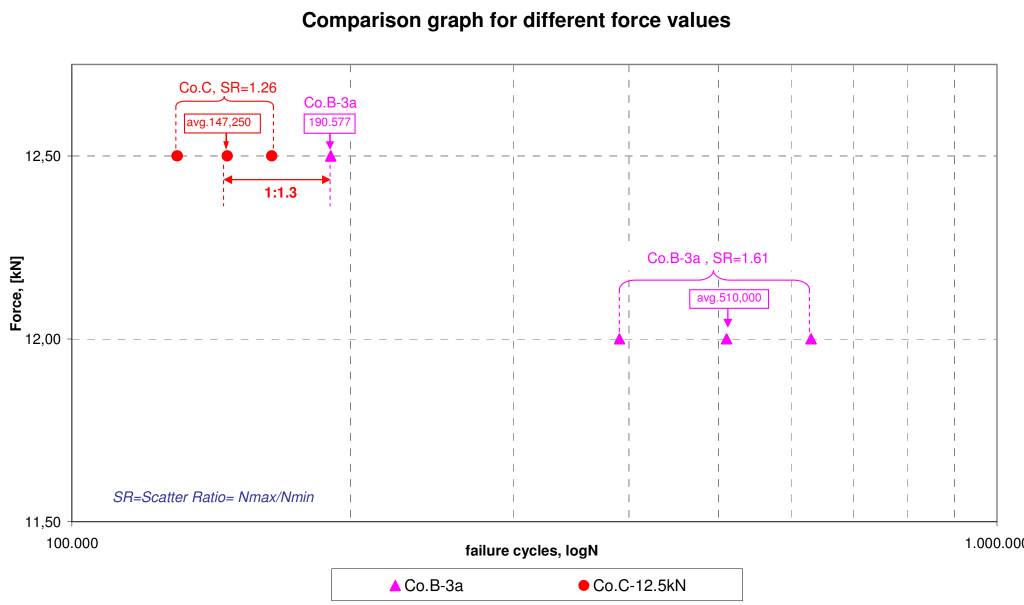

Figure 5.18: Comparative graph for 12-12.5 kN.

5.12 OTHER CRITERION

Stiffness is another evaluation criterion. According to the technical drawing value, theoretical stiffness is around 155N/mm. The tests have shown that the averaged stiffness value for Co.A-50CrV4 is 146N/mm, for Co.A-61SiCr7 is 144N/mm and for Co.B-51CrMoV4 is around 150N/mm. It is a well-known fact that stiffness [a,*] has a positive effect on the fatigue life of the component force controlled conditions.

Throughout the tests, both the place of fracture and the fractured surface of the bars have also been evaluated.When the FEA [b,*] is examined, the most critical place on the stabilizer bar with respect to the stress is on the bend. The test results have shown that the places of fracture in Co.B samples are mainly away from the bend. And also the fatigue lines seen on the surface of the fractured bar show a clear expression of the fatigue mechanism, see Figure 42. These figures display that in some of Co.B samples the fracture starts from the inside which is the indication of homogeneous material, good surface finish and therefore longer fatigue life.

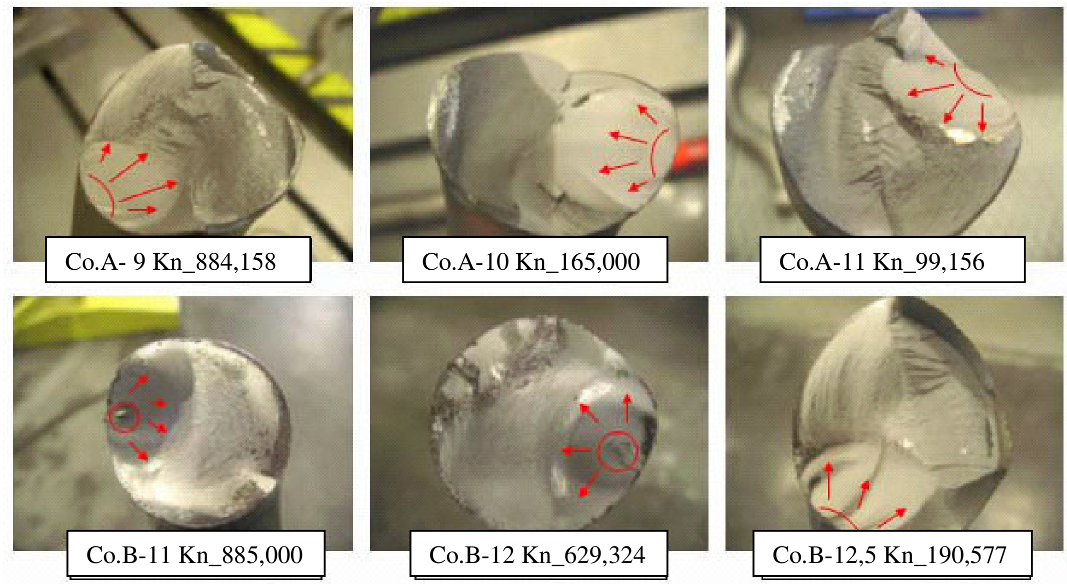

Figure 5.19: Fractured surfaces of the samples.

a. See: Theoretical Methods, Stiffness
b. FEA: Final Element Analysis, see Experimental Methods for FEM and ANSYS

Often a characteristic form of the crack initiation is to be observed underneath the wire Surface. Thus, a clear centre of crack initiation which possibly corresponds to one or more grain boundary areas arranged in nearly the same position is discernible at a depth of approximately one tenth of a millimetre. A possible failure mechanism to be assumed here – subject to further extensive examinations – is that a „gaping" of the grain boundaries is taking place which leads to a first microcrack. This small crack then propagates further because of the high stress amplitude and eventually leads to the fracture of the spring. [10]

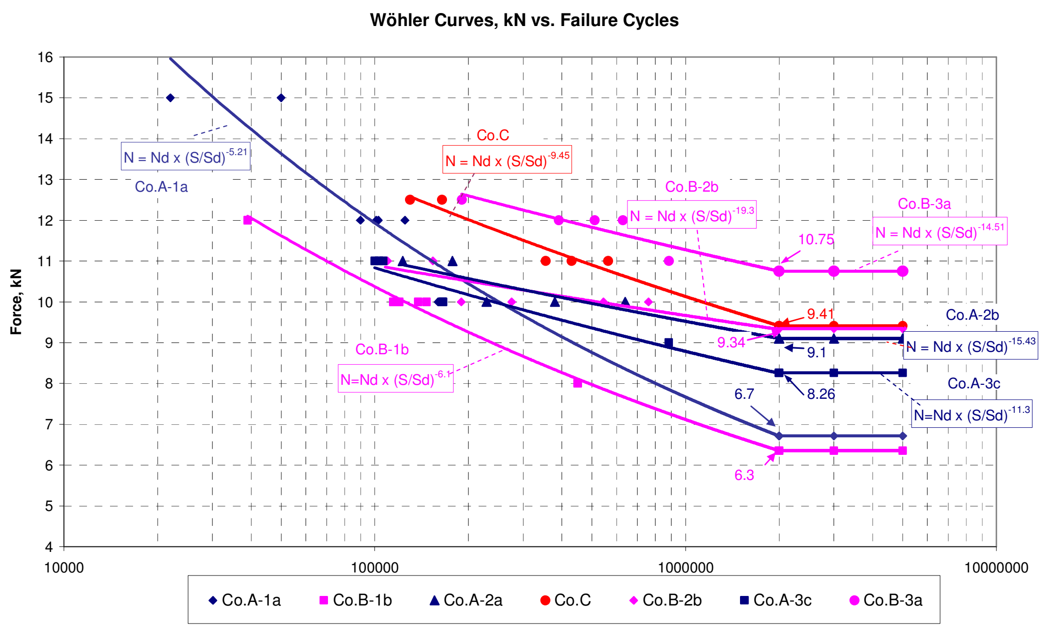

Figure 5.20: Overall Wöhler Lines (a,b,*).

---

[10]: [citation from "Fatigue Behavior of Technical Springs" written by B. Kaiser, C. Berger]
a. "Overall Wöhler Lines" graph is attached to the App.A Section in a larger format, See Fig A.1
b. Also see Figure A.2 for the comparison graph of forces related to the Wöhler Curves

5.13 EXPERIMENTS SUMMARY

Results obtained show that Co.B with its new material proposal, 51CrMoV4, is the most durable one between Co.A and Co.C substitutes.

Co.B-51CrMoV4 has the highest stiffness value. Co.A with 61SiCr7 material does not not give satisfactory results. The tests of Co.B-50CrV4 with Boron additives will be carried out by Co.B itself.

Scatter in both Co.B and Co.A samples has greatly decreased as it seen on the Figure 5.20 above.

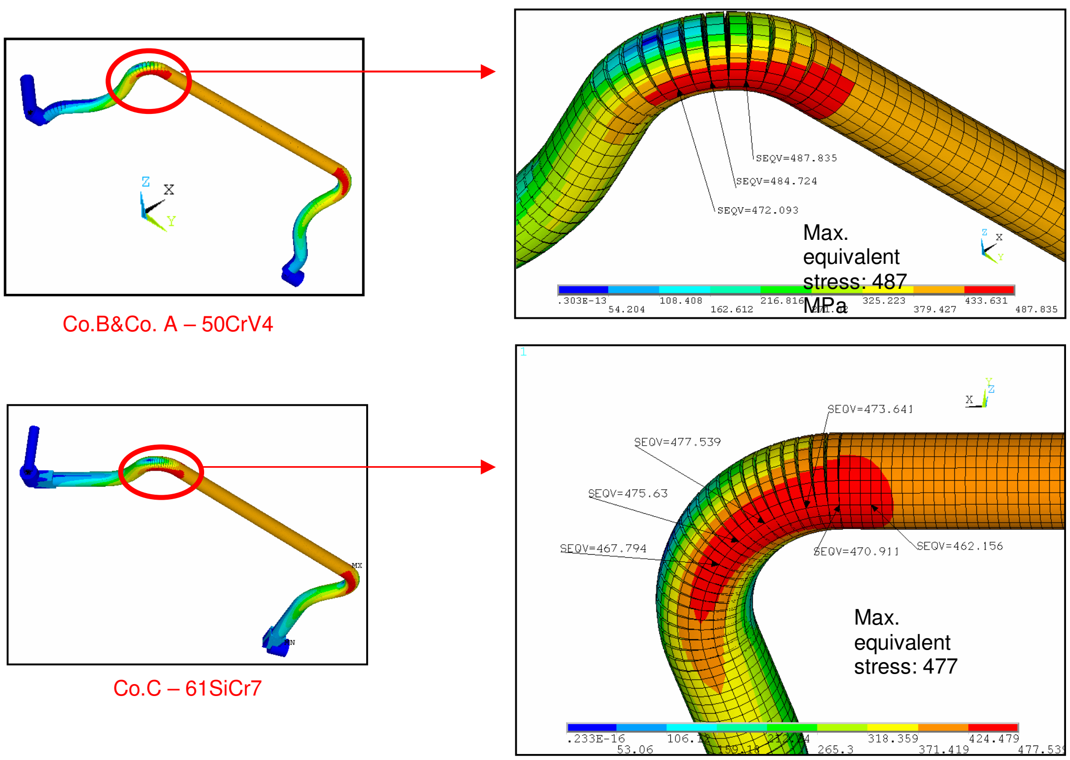

Figure 5.21: FEA Results of the specimens

With the new production process (new bending machine), Co.A is the best one but with a cost of durability. Failure points in Co.A is always on the bending part of the bar. But that of Co.B is mainly away from that part. Figure 5.21 shows the FEA results of the three samples. Fraction points are obviously marked with the meshed areas in red.

Experiment history could be organized briefly as following:

5.13.1 SPECIMEN in GROUPS

First group was consisting of Co.A Serial – 50CrV4 and Co.B – 50CrV4 (prototype fixture). Obtained results were unsuccessful because of the low durability.

Second group was consisting of shot peened Co.A – 50CrV4 sample, serial fixtured and shot peened Co.B – 50CrV4 sample and Co.C – 61SiCr7 with its new geometrical form. Obtained results were partly acceptable, if both Co.C with high durability and Co.A and Co.B with high scattered values are excepted.

Finally third group of experimental series was consisting shot peened Co.A – 61SiCr7 samples produced with a new bending technique, shot peened Co.A – 50CrV4 samples also bent with a new maschine, Co.B – 51CrMoV4 samples and at last Co.B – 50CrV4+ sample including Boron additives. Performance of Co.B 50CrMoV4 sample has reached a high satisfaction. At Figure 5.20, the pink line at the top represents these results.

Remarkable improvements of the fatigue properties of stabilizers at tests were achieved by shot peening.

“ Shot peening involves tensile plastic deformation of a surface layer – produced as a sum of numerous indentation expansions. Compressive residual stresses are generated at the surface because of this tensile deformation. Peening can impose huge amounts of deformations without cracking because of the hydrostatic compression that is involved.

The level of surface compressive residual stress is approximately half of the yield strength for the heavily work-hardened surface. This “skin” has a thickness that is largely determined by the size of the shot particles that have been used. Residual and applied stress superimpose themselves, so that compressive surface residual stresses offset tensile applied surface stresses. It is that lowering of net surface stress that improves the service performance of shot peened components.” [10]: **B. Kaiser, C. Berger**, 2005.

[10]: [citation from “Fatigue Behavior of Technical Springs” written by B. Kaiser, C. Berger]

All in all innovations of competitor companies at their production techniques and optimizations they made at the mechanical such as chemical properties of specimens [a,*] contribute a better quality. Experiments also technically proved that Co.B is a convenient substitute of Co.A.

Co.C with its remarkable results demonstrates only a good work of design, which is unfortunately not suitable for the tested vehicles suspension system. Another important conclusion is the importance of using materials innovated with the new chemical knowledge.

5.13.2 FEM ANALYSIS – DETAILED EXPLANATION

A comparison of experimental results were always made with hand calculations. Today researchers and engineers got the opportunity proving experimental results with multiple softwares specified for scientific analysis. These softwares are innovated in order to approximate the experimental data via mathematical analysing methods like FEM. One of the most common used softwares is ANSYS like mentioned at former chapters.

How those colored graphs are done in computer and how the data is calculated ? Following section [b,*] includes screen shots picked up from the computer during the analysis to explain the infrastructure of the experiment.

The data collected with strain gages are also depicted on a graph in order to compare ANSYS calculated stress/strain values with the experimental results.

---

a. See Table A.6 at the Appendix section for the material properties of all Stabilizer specimen
b. See FEM Section – Chapter 6

6 FEM SECTION – STRUCTURAL ANALYSIS in STEPS

Following screen shots are obtained from ANSYS software. In order to start with an new analysis, it's a must to having a three dimensional solid model. 3D samples can be obtained by using a CAD software. After drawing the model, it can be easily imported into analysing software, however the 3D visuals can be drawn via ANSYS like samples mentioned below.

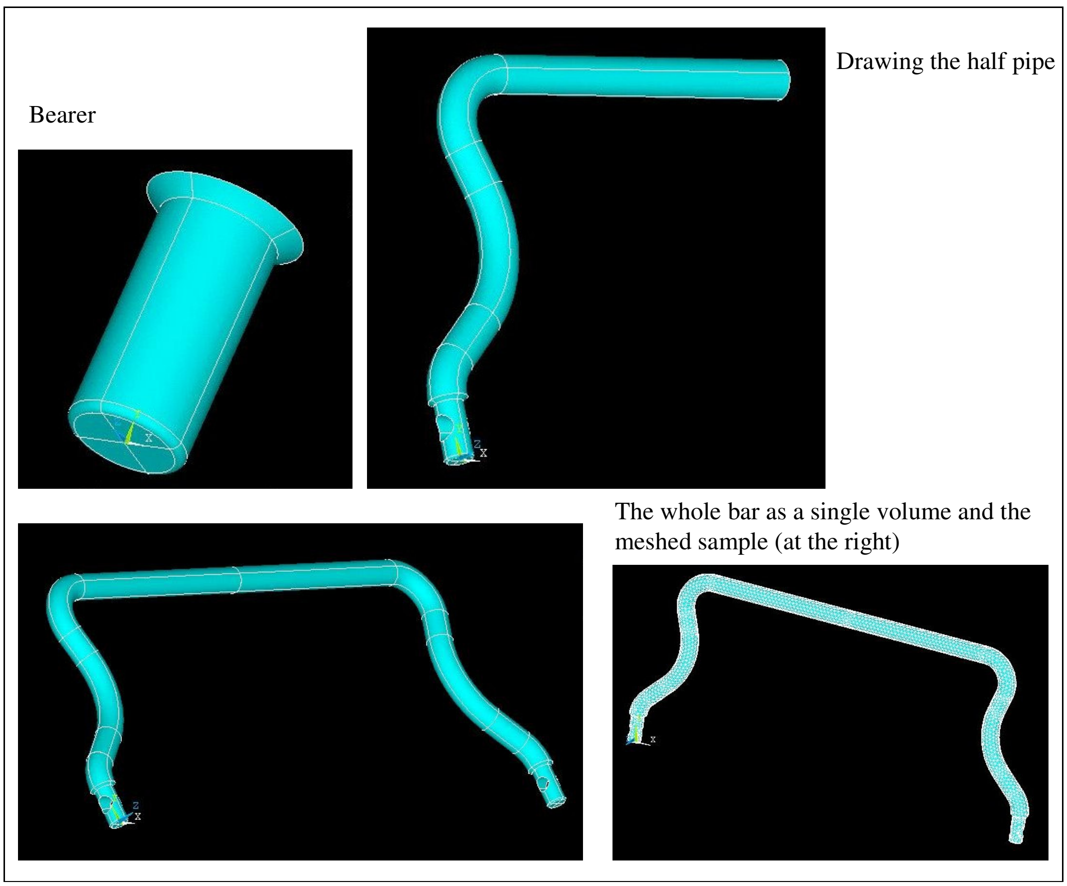

Figure 6.1: 3D modelling samples in ANSYS.

6.1 PREPROCESSING: DEFINING the PROBLEM

Main steps are listed below to make structural analysis with ANSYS [7]: **Cook, Robert Davis,** 1995:

1. Modeling (Creating the solid model with utilities in software [(a,*)] or outsourcing the file)
2. Defining the element type (Solid 90 in this case)
3. Defining the geometrical properties (like outside diameter, thickness of walls etc. – not a necessary variable for this type of solid element)
4. Specifying the material properties (structural>linear>elastic>isotropic and E=210.000 N/mm², ν=0.3 [(b,*)])
5. Meshing the volume [(c,*)]
6. Assigning loads and constraints (Applying Displacement/Force/Moment on Keypoints)
7. Solving the system (Deflection/Stress/Strain data etc. will be calculated with PC)

After obtaining the results using ANSYS, Deformed Shapes and Nodal Results can be listed in text format or depicted in various graphs according the requested parameters like (von Misses Stress etc.). Complex geometries used today require high accuracy in results. Analyzer-calculated results are much more precise than hand-calculated ones and they also can be obtained very quickly. Therefore, every engineer should be capable to analyze with similar tools instead of making hand calculations. Figures 6.2 and 6.3 are depicting the deflection and stress values on the stabilizer bar forced with 10 kN at one end.

---

a. E is the default value of Young's Modulus for hardened steel and ν however is Poisson's Ratio related to material
b. The Volumes are based on many keypoints located in space. These keypoints are getting connected through lines and crossectional areas which are actually guiding the software to generate the single volume.
c. Creating arbitrary geometries on the surface to set noddle points. FEM is based on matrisses including numerous noddle points. See Theoretical Methods for details.

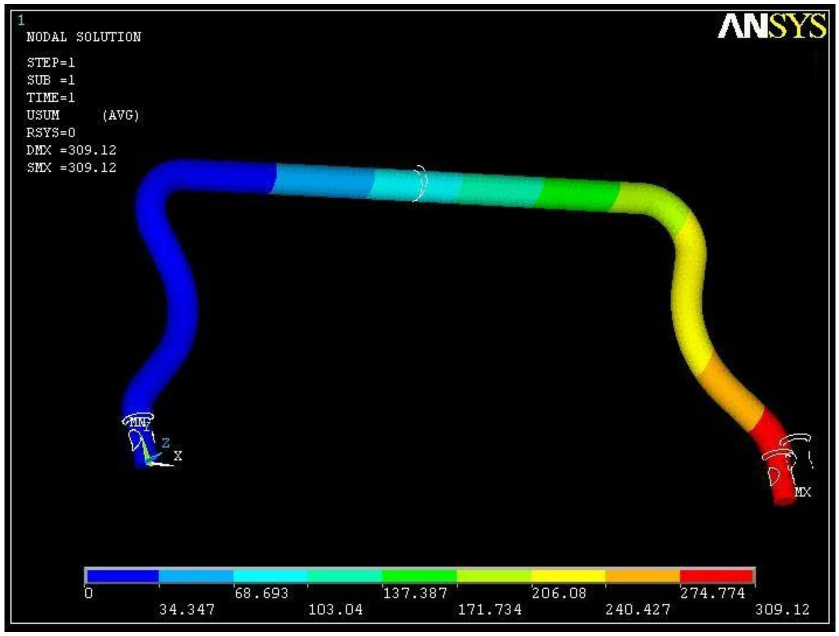

Figure 6.2: Deflection Analysis of Stabilizer Bar [(a,*)].

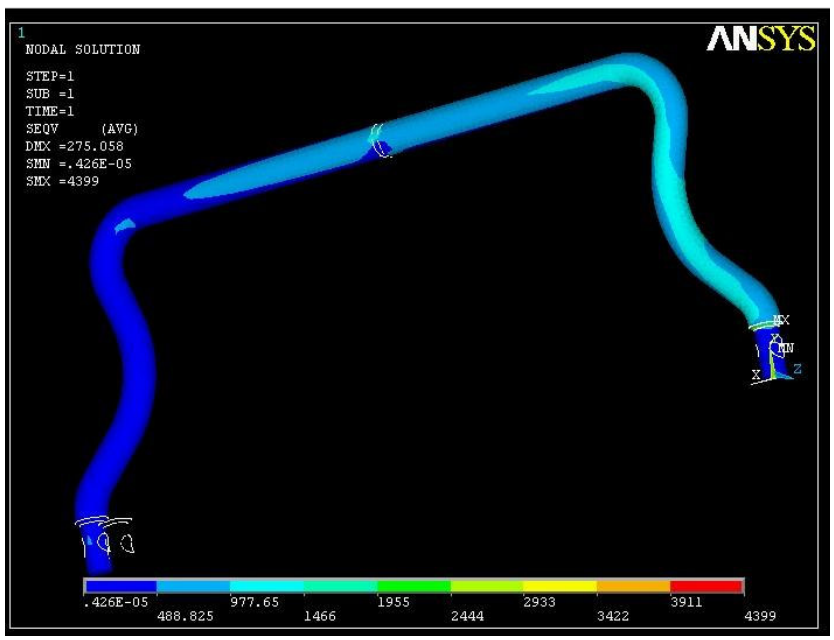

Figure 6.3: Stress Analysis of Stabilizer Bar [(b,*)].

a. Deflection varies values between 0 and 309 mm in z direction.
b. Stress values get the highest mark at the areas turning into red color, about 4000 MPa in this case.

6.2 PROBLEM DESCRIPTION

The problem to be solved in this example is the analysis of a stabilizer bar. The problem to be modeled in this example is simply showed in the following figure. The bar is to be built of hardened [(a,*)] steel tubing (full) having an outside diameter of 45 mm. The Bar is fixed on all directions at one end and forced with 10 to 13 kN at the free end. In order to prevent rotating on its own axis, the stabilizer bar is also fixed with bushings [(b,*)].

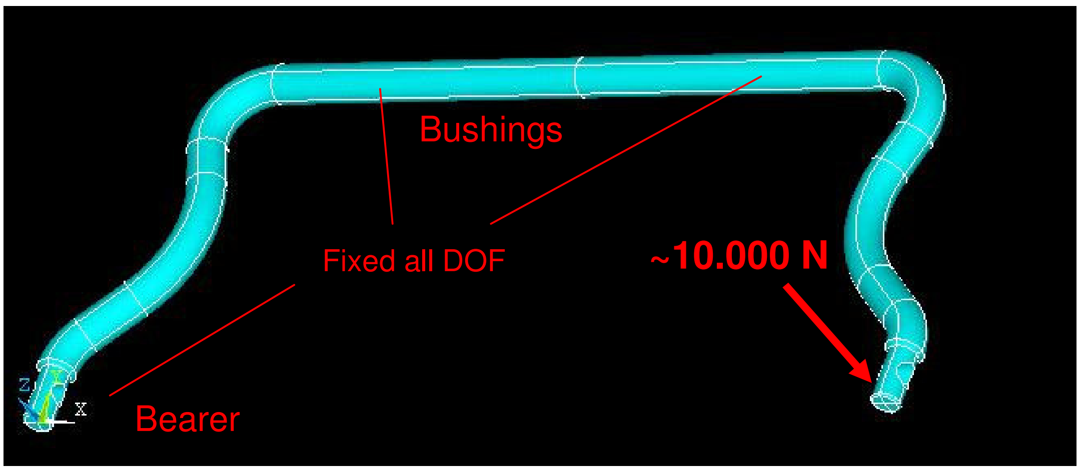

Figure 6.4: Experiments Infrastructure

6.3 POSTPROCESSING: VIEWING the RESULTS

After calculations using ANSYS, it is possible to find a variety of options to deal with.

1. Plotting results of deformed shape (to view both the deformed and undeformed object
2. Observing the value of the maximum deflection (which must be identical to that obtained via hand calculations[(c,*)])
3. Plotting nodal solutions – DOF Solution (This means that a listing off all translational or rotational degrees of freedom from the solution)

---

a. Shot peened – See Theoretical Methods.
b. See pics at Experimental Methods to see real pics. A simple demonstration is at Fig.6.4 above.
c. Not easy for this case because of the high accuracy (intensive meshed area)

4. Deriving data via Element Table and listing (like stesses, strains)
5. Further actions to verify obtained data of the model

At the following screen shot (See Fig.6.4) some equivalent stress values at the critical areas (like bending curve) are depicted according ANSYS calculations. ANSYS allows to plot a variety of parameters in graphs and numbers. They could be stress, strain and deflection values (See App.C for various ANSYS screen shots).

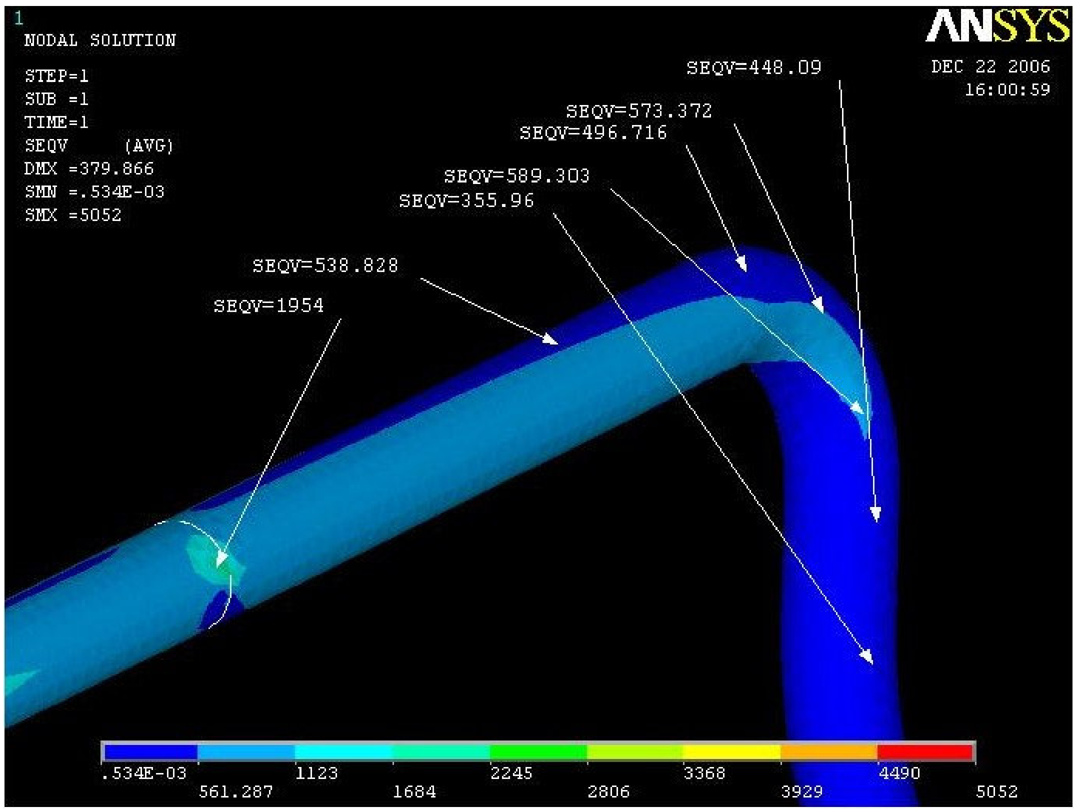

Figure 6.5: Equivalent Stree Values by Bending

7 SOLUTION and DISCUSSIONS

7.1 VERIFYING ANSYS CALCULATIONS with TEST RESULTS

Unfortunately making a very healty match isn't possible. This problem could be considered under heading of "Fatigue Behaviour Calculation under Extreme Forces" (according the hypothesis called "Linear Shape Change Energy") [6]: **Feodosiev, V. I. (Vsevolod Ivanovich),** 2005.

In english, verifying the results could be done through a few formula using the tubes dimensions. The table beneath simplyfies the verification in steps.

Default values are also included in formulas in order to calculate material specific (See Fig.7.1 for picked values of dimensions at fracture point).

Table 7.1: Comparison Stress Calculation

F = 12 kN	**Nfract.**	**=102,800 (from the loadside)**			
Material Specifications :					
Material :	**(M)**	50CrV4	(Ø = 45cm)		
Fracture Point :	**(σf)**	900-1000 N/mm2			
Bending Yield Point:	**(σby)**	750 N/mm2			
Torsional Yield Point:	**(σty)**	500 N/mm2			
Moment of Inertia	**(I)**	= (π/4)/r^3=	8946,176		[mm3]
Polar Moment of Inert.	**(J)**	= 2 x I =	17892,352		[mm3]
Fracture Point					
Vertical Distance to the point of loading			=	420	mm
Horizontal distance to the point of loading			=	90	mm
Torsion	(τ)	= T.c / J =	**281,68**	[N/mm2]	
Bending Moment	(σA)	= M.c / I =	**120,72**	[N/mm2]	
Comparison Stress	(σV)	= (σA2 + 3. τ2)1/2 =	**502,61**		[N/mm2]

Comparing the result with random picked stress values from ANSYS screen (See Fig.6.5), it can be clearly seen that the results are compable. FEM approximation was successfull with results about 500 N/mm² like expected. Evaluation can go further by picking similar points over surface and matching the results.

Figure 7.1: Stabilizer Bar – Vertical and horizontal distances of fracture point from the axis of movement (used in formula, See Table 7.1)

According experiment reports fractures mostly occured at these bending points. However the stress graphs shows that there other critical areas like the middle of the bar or bearers.

The endurance of a structure is up to three technical issues.

- Geometrical design
- Manufacturing skills
- Chemical properties of raw material

At this work, all of them are evaluated step by step and the behaviour of the stabilizer bar is described in each case if there is an innovation or difference between both former sample and the present one. FEM approximation was useful to determine stress distribution over the stabilizers surface under torsion and it was also helpful to imagine the circumstances abroad. With the help of an analysing software like ANSYS, the car suspension system and its related parts can be observed in numerous ways from different techical aspects.

BIBLIOGRAPHY

[1] **Hurd, N.J.,** 1996. Torsional performance of driveshafts for vehicle driveline applications, Warrendale, PA : Society of Automotive Engineers. (Page: 26)

[2] **Russell A. Chernenkoff, John J. Bonnen,** 1997. Recent developments in fatigue technology, Warrendale, PA : Society of Automotive Engineers. (Page: 15)

[3] **Case, John, Lord Chilver, Carl T.F. Ross**, 1993. 1888 - 1969 Strength of materials and structures: with an introduction to finite element methods, Edward Arnold. (Page: 16)

[4] **Bijen, Jan,** 2003. Durability of engineering structures : design, repair and maintenance, Boca Raton : CRC ; Cambridge : Woodhead. (Page: 17)

[5] **Budynas, Richard G. (Richard Gordon),** 1999. Advanced strength and applied stress analysis, Boston : WCB/McGraw-Hill. (Page: 19)

[6] **Feodosiev, V. I. (Vsevolod Ivanovich),** 2005. 1916 - Advanced stress and stability analysis : worked examples / V.I. Feodosiev ; translated by S.A. Voronov and S.V. Yaresko, Berlin : Springer. (Page: 61)

[7] **Cook, Robert Davis,** 1995. Finite element modeling for stress analysis, New York : Wiley. (Page: 57)

[8] **Piper, D. E,** 1970. Standardization of test methods for stress-corrosion cracking, [Neuilly-sur-Seine, France] : North Atlantic Treaty Organization. (Page: 32)

[9] **Tada, Hiroshi, Hiroshi Tada, Paul C. Paris, George R. Irwin,** 2000. The stress analysis of cracks handbook, [Neuilly-sur-Seine, France] : North Atlantic Treaty Organization. (Page: 30)

[10] **B. Kaiser, C. Berger**, 2005. Fatigue behaviour of technical springs, Institute for Materials Technology and State Materials Testing Institute Darmstadt University of Technology, Darmstadt, Germany. (Pages: 52 and 54)

[11] **A. Rinaldi, P. Peralta, D. Krajcinovic, Y.-C. Lai,** 2005. Prediction of scatter in fatigue properties using discrete damage mechanics, Arizona State University, USA. (Page: 37)

[12] **DIN 50100**, Feb.1978. Fatigue Testing Standart, Continuous Vibration Test, *DIN Deutsches Institut für Normung e.V.,* Berlin. (Page: 7)

[13] **mts.com,** Manufacturers offical web site, Hydropuls Testing Units. (Page: 27)

APPENDIX A : TABLES and FIGURES of EXPERIMENTS

Table A.1: Test Results of Experiment 1

Type	Specimen	Test No	Min.Force F_u (kN)	Max. Force F_o (kN)	Amplitude F_{ampl} (kN)	Resultant Stress 6v (N/mm2)	Stiffness (N/mm) (Cs)VA=155 (Cs)HA=132	Freq.	Number of cycles N in 10^6	Number of cycles o;x	Type of fracture	Place of fracture	Duration (min)
Front axle	Co.A Serial	1	-14,80	15,00	14,90	666,44	167,68	1,0	22000	x	shear fracture	near bushing	367
		2	-14,80	15,00	14,90	693,50	161,14	1,0	50000	x	shear fracture	near bushing	833
		3	-10,00	10,00	10,00	448,76	167,13	2,0	160000	x	shear fracture	near bushing	1333
		4	-11,80	12,00	11,90	498,61	179,00	1,0	125000	x	brittle fracture	on the bend	2083
		5	-11,80	12,00	11,90	472,48	188,90	1,0	90000	x	brittle fracture	on the bend	1500
		6	-10,00	10,00	10,00	-	-	1,5	>1000000	o	no fracture	-	11111
		7	-12,10	12,20	12,15	538,51	169,22	1,0	101161	x	shear fracture	near bushing	1686
		8	-12,10	12,10	12,10	502,61	180,56	1,0	102800	x	shear fracture	on the bend	1713
	Co.B Prototype	1	-11,80	12,00	11,90	587,10	152,02	1,0	39000	x	shear fracture	on bushing	650
		2	-9,90	10,10	10,00	450,00	166,67	1,0	120000	x	brittle fracture	on the bend	2000
		3	-9,95	10,15	10,05	477,88	157,73	1,0	115000	x	brittle fracture	on bushing	1917
		4	-8,00	8,05	8,03	350,00	171,96	2,0	450000	x	shear fracture	on bushing	3750
		5	-8,00	8,05	8,03	-	-	2,0	>1500000	o	no fracture	-	12500
		6	-10,00	9,95	9,98	408,00	183,36	1,5	146735	x	brittle fracture	on the bend	1630
		7	-10,15	10,15	10,15	387,86	196,27	1,5	50000	x	brittle fracture	on the bend	556
		8	-10,15	9,95	10,05	500,00	150,75	1,5	138000	x	shear fracture	btw bushing	1533
Rear axle	Co.A Serial	1	-12,70	12,00	12,35	488,00	168,29	1,0	198551	x	shear fracture	near bushing	3309
		2											
		3											
	Co.B Prototype	1	-12,82	12,00	12,41	609,95	135,30	1,0	42851	x	shear fracture	btw bushing	714
		2											
		3											

x: specimen broken; o: specimen not broken; (dotted shading): ignored test

Table A.2: Test Results of Experiment 2

Type	Specimen	Test No	Amplitude F_{ampl} (kN)	Freq.	Number of cycles N in 10^6	o;x	Place of fracture
Front Axle	Co.A	1	10,00	2,0	160000	x	near bushing
		2	10,00	1,5	1000000	o	no fracture
		3	12,00	1,0	125000	x	on the bend
		4	12,00	1,0	90000	x	on the bend
		5	12,00	1,0	101161	x	near bushing
		6	12,00	1,0	102800	x	on the bend
		avg.	12,00	-	104740	-	-
		7	15,00	1,0	22000	x	near bushing
		8	15,00	1,0	50000	x	near bushing
	Co.B	1	8,00	2,0	450000	x	on bushing
		2	8,00	2,0	1500000	o	no fracture
		3	10,00	1,0	120000	x	on the bend
		4	10,00	1,0	115000	x	on bushing
		5	10,00	1,5	146735	x	on the bend
		6	10,00	1,5		x	on the bend
		7	10,00	1,5	138000	x	btw bushings
		avg.	10,00	-	129934	-	-
		8	12,00	1,0	39000	x	on bushing
	Co.B (reinforced)	1	10,00	1,0	276000	x	on the bend
		2	10,00	1,0	760000	x	btw bushings
		3	10,00	1,0	190000	x	on the bend
		4	10,00	1,0	545000	x	on the bend
		avg.	10,00	-	442750	-	-
		5	11,00	1,0	108000	x	on the bend
		6	11,00	1,0	110000	x	btw bushings
		7	11,00	1,0	154000	x	on the bend
		avg.	11,00	-	124000	-	-
	Co.A (shot-peened)	1	10,00	1,0	229000	x	on the bend
		2	10,00	1,0	380000	x	on the bend
		3	10,00	1,0	639000	x	on the bend
		avg.	10,00	-	416000	-	-
		4	9,00	1,0	1000000	o	no fracture
		5	11,00	1,0	122960	x	on the bend
		6	11,00	1,0	178000	x	on the bend
		avg.	11,00	-	150480	-	-
	Co.C	1	11,00	1,0	430000	x	on the bend
		2	11,00	1,0	564000	x	on the bend
		3	11,00	1,0	355000	x	on the bend
		avg.	11,00	-	449667	-	-
		4	12,50	1,0	164500	x	on the bend
		5	12,50	1,0	130000	x	on the bend

Table A.3: Test Results of Experiment 3 (Co.A & Co.B)

Type	Specimen	Test No	Weight (kg)	Amplitude (kN)	Displacement (mm)	Stiffness (N/mm)	Frequency (Hz)	Number of cycles N in 10^6	Number of cycles o;x	Place of fracture
Front Axle	Co.A - 61SiCr7	1	21,94	11,00	not measured		1,0	69484	x	on the bend
		2	21,98	12,00	± 83,465	143,00	1,0	52300	x	on the bend
		3	22,00	11,00	not measured		1,0	74645	x	on the bend
		4	22,00	11,00			1,0	51666	x	on the bend
		5	22,00	10,00	± 69,005	145,28	2,0	49800	x	on the bend
	Co.A - 50CrV4	1	22,24	11,00	± 76,71	143,39	1,0	106631	x	on the bend
		2	22,24	11,00	± 75,285	146,28	1,0	99156	x	on the bend
		3	22,22	10,00	± 68,51	146,55	1,0	165000	x	on the bend
		4	22,24	10,00	± 68,4	146,2	1,0	165784	x	on the bend
		5	22,22	9,00	± 62,36	144,25	2,0	884158	x	on the bend
	Co.B - 51CrMoV4	1	22,18	11,00	± 72,82	151,41	1,0 - 2,0	885100	x	near bushing
		2	22,22	12,00	± 79,79	150,61	1,0	390823	x	on the bend
		3	22,22	12,00	± 80,475	149,10	1,0	629374	x	on the bushing
		4	22,20	12,00	± 82,995	150,63	1,0	190577	x	on the bend
		5	22,20	11,00	± 76,76	150,53	1,0	191365	x	in the middle
	Co.B - 50CrV4 (with Boron additives)	1	tested by Co.C itself							
		2								
		3								
		4								
		5								

Table A.4: Overall Test Results

Samples	Process	Material	8 kN	9 kN	10 kN	11 kN	12 kN	12,5 kN	15 kN
Co.A	serial	50CrV4			160000		125000		22000
							90000		50000
							101161		
							102800		
	shot peened	50CrV4		1000000	229000	122960			
					380000	178000			
					629000				
	shot peened machine	50CrV4		884158	165000	106631			
					165784	99156			
	shot peened	61SiCr7			49800	69484	52300		
						51666			
						74645			
Co.B	shot peened with prototype fixture	50CrV4	450000		115000				
			1500000		120000				
					146735				
					138000				
	shot peened with serial fixture	50CrV4			276000	108000			
					760000	110000			
					190000	154000			
					545000				
	shot peened	51CrMoV4				885100	390823	190577	
							629374		
	shot peened with reinforcing additives	50CrV4+	tested by Co.B itself						
Co.C	new form	61SiCr7				430000		164500	
						564000		130000	
						355000			

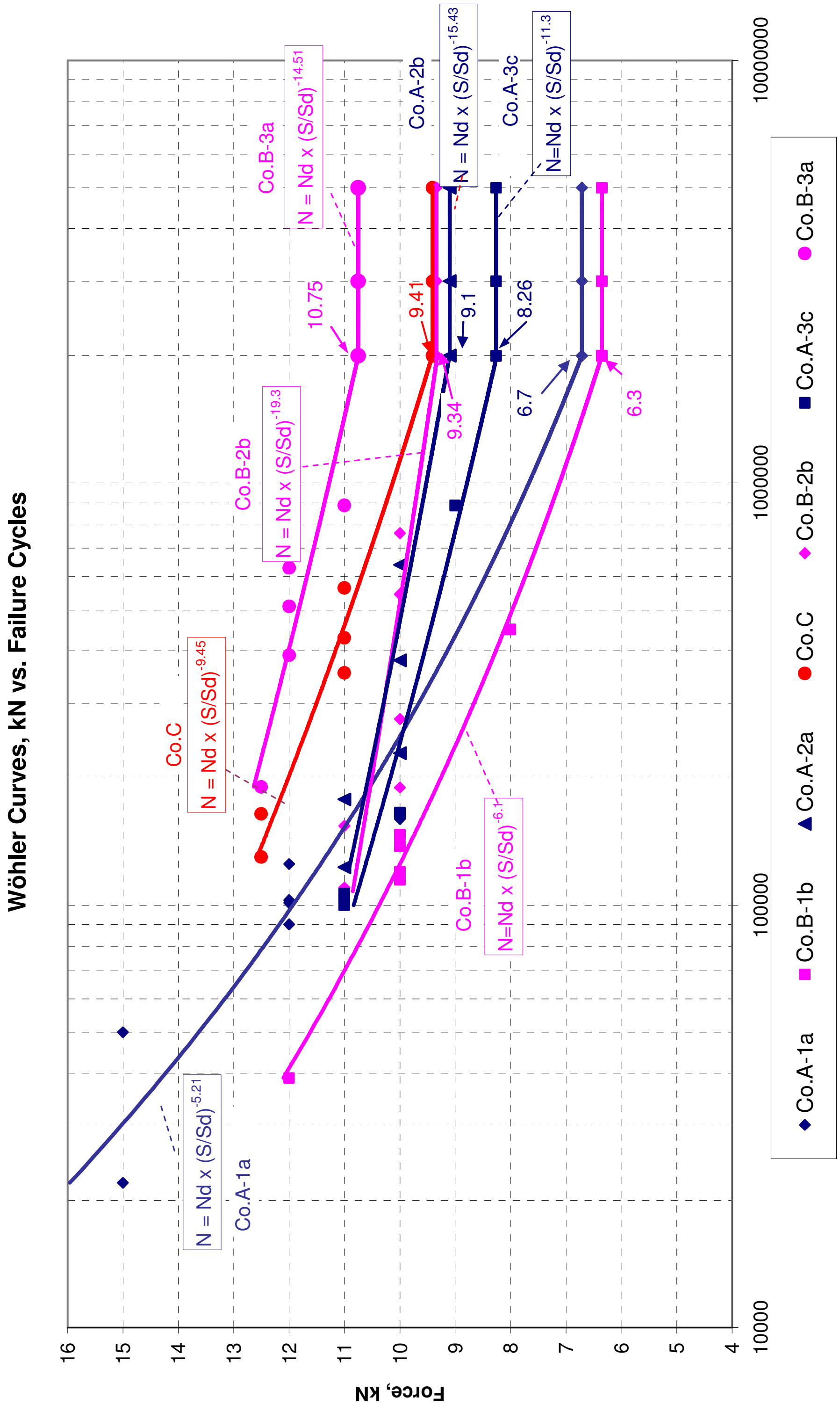

Figure A.1: Comparative Wöhler Curves vs. Failure Cycles

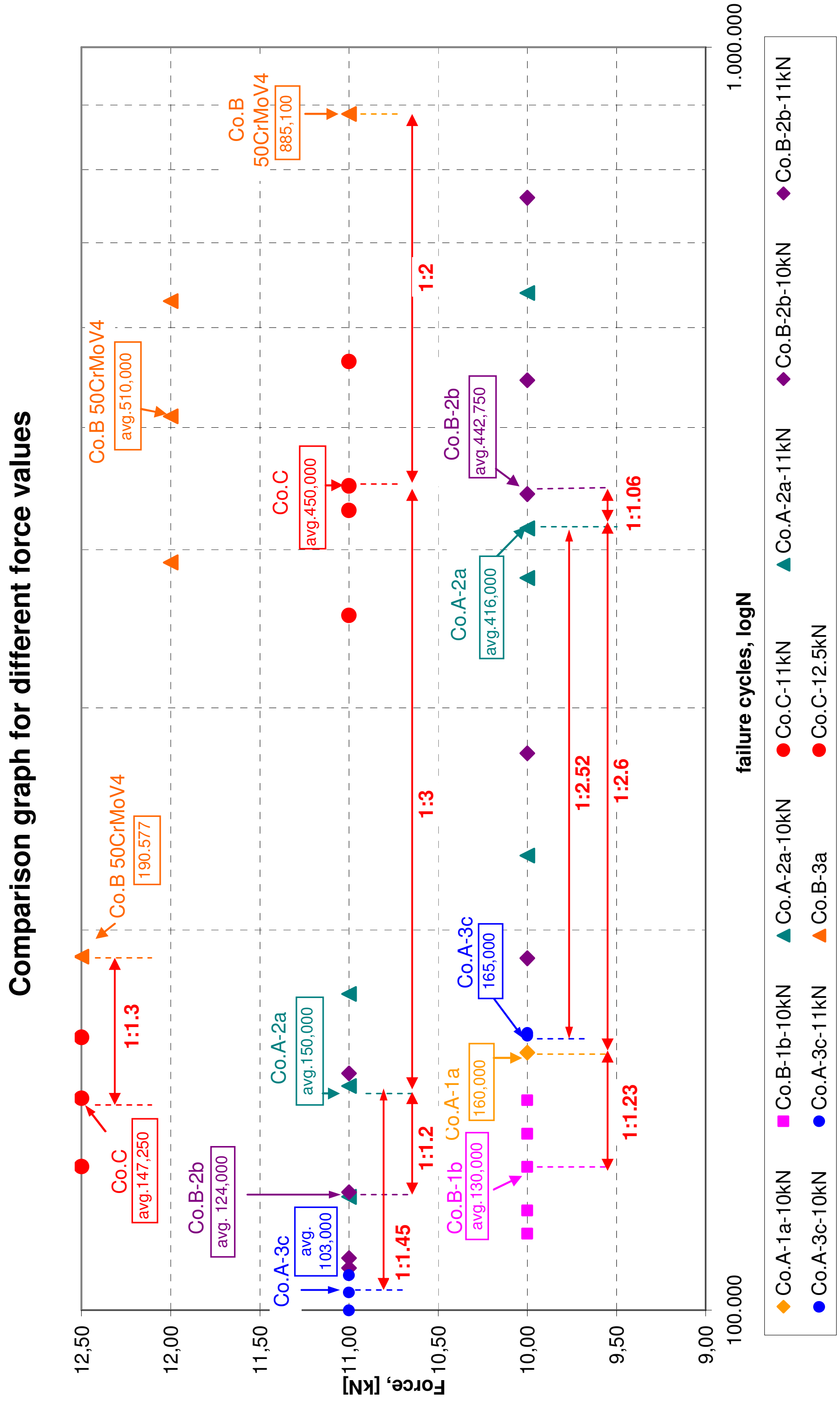

Figure A.2: Comparative Graph for different force values

Table A.5: Material Properties of Stabilizer Specimen

Material UMS03.01 (60SiCr8) 45mm dia.
Material E=210000NPa $б_{yield}$=900MPa d=783

	Weight (Kg)	Material	Chemical Analysis – Specification (wt %) C	Mn	Si	P	S	Cr	Mo	V	Cu	Ti	Sn
Accepted Values	22529	50CrV4	0,47	0,50	0,04	0,025	0,025	0,80		0,10			
			0,55	0,80	max.	max.	max.	1,20		0,25			
Accepted Values	23900	61SiCr7	0,57	0,70	1,60	0,025	0,025	0,20					
			0,65	1,00	2,00	max.	max.	0,45					
Accepted Values	23900	51CrMoV4	0,48	0,70	0,4	0,025	0,025	0,90	0,15	0,10			
			0,56	1,10	max.	max.	max.	1,20	0,30	0,20			
Co.B_Prot. (Measured at labor)	21700	50CrV4	0,48	0,74	0,235	0,018	0,004	1,10	0,026	0,13	0,227		
Co.B_Prot. (Measured at Co.B)		50CrV4	0,5071	0,7011	0,232	0,018	0,001	1,08	0,027	0,128	0,1987	0,0032	0,0153
Co.A	22540	50CrV4	0,517	1,01	0,28	0,013	0,008	1,10	0,003	0,1	0,03		
Co.B_serially fixtured	22040	50CrV4	considered to be the same as the former one										
Co.A - shot peened	22460	50CrV4	not measured yet										
Co.C	23340	61SiCr7	0,64	0,98	1,65	0,012	0,019	0,37	0,015				
Co.B 51CrMoV4	22220	51CrMoV4	0,5	0,8	0,3	0,01	0,00	1,25	0,17	0,09			

APPENDIX B: TABLES of CHEMICAL PROPERTIES

Table B.1: Material specification sheet of 50CrV4

Saarstahl - 51CrV4 (50CrV4)

Material No.:	Former brand name:	International steel grades:
1.8159	**F2K**	**BS:** 735A51, 735M50, 735H51 **AFNOR:** 50CrV4, 51CV4 **SAE:** 4150

Material group: Steel for quenching and tempering according to DIN EN 10083

Chemical composition: (Typical analysis in %)	C	Si	Mn	Cr	V	other
	0,50	0,25	0,90	1,10	0,12	(Pb)

Application: Alloyed heat treatable steel with a typical tensile strength of 900 - 1200 N/mm². For automotive and mechanical engineering components as gear parts, pinions, shafts.

Hot forming and heat treatment:

Forging or hot rolling:	1050 - 850°C
Normalising:	870 - 900°C/air
Soft annealing:	680 - 720°C/furnace
Hardening:	820 - 860°C/oil
Tempering:	540 - 680°C/air

Mechanical Properties:

Treated for cold shearability +S:	See condition A
Soft annealed +A:	max. 248 HB

Quenched and tempered, +QT:

Diameter d [mm]	< 16	>16 – 40	>40 – 100	>100 – 160	>160 – 250
Thickness t [mm]	< 8	8<t<20	20<t<60	60<t<100	100<t<160
0,2% proof stress $R_{p0,2}$ [N/mm²]	min. 900	min. 800	min. 700	min. 650	min. 600
Tensile strength R_m [N/mm²]	1100 - 1300	1000 - 1200	900 - 1100	850 - 1000	800 - 950
Fracture elongation A_5 [%]	min. 9	min. 10	min. 12	min. 13	min. 13
Reduction of area Z [%]	min. 40	min. 45	min. 50	min. 50	min. 50
Notch impact energy ISO-V [J]	min. 30	min. 30	min. 30	min. 30	min. 30

Table B.2: Material specification sheet of 51CrMoV4

Saarstahl - 52CrMoV4 (51CrMoV4)

Material No.:	Former brand name:	International steel grades:
1.7701	**F4K**	**BS:** **AFNOR:** 51CDV4 **SAE:**

Material group:	Hot rolled steel for springs suitable for quenching and tempering according to DIN 17221

Chemical composition: (Typical analysis in %)	C	Si	Mn	Cr	Mo	V
	0,50	0,25	0,90	1,10	0,25	0,10

Application:	Hot rolled steel for springs for highly strained springs suitable for quenching and tempering, as leaf springs and helical vehicle springs, stabilisers vehicle, torsion bars, cup springs.

Hot forming and heat treatment:		
	Hot forming:	1050 - 850°C
	Hot deformation:	920 - 830°C
	Normalising:	850 - 880°C/air
	Soft annealing:	640 - 680°C/furnace
	Hardening:	830 - 860°C/oil
	Tempering:	430 - 500°C/air

Mechanical Properties:		
	Treated for cold shearability +S:	max. 280 HB
	Soft annealed +A:	max. 248 HB
	Spheroidized annealed - GKZ (+AC)	max. 225 HB
	Core hardness after quenching:	min. 54 HRC

	Hardened and tempered, H+A, 16 mm flat steel bars, 25 mm bars
0,2% proof stress $R_{p0,2}$ [N/mm²]	min. 1200
Tensile strength R_m [N/mm²]	1400 - 1700
Fracture elongation A_5 [%]	min. 6
Reduction of area Z [%]	min. 30
Notch impact energy ISO-V [J]	min. 6

Table B.3: Material specification sheet of 61SiCr7

Saarstahl - 61SiCr7 (60SiCr7)

Werkstoff-Nr.:	Alte Werksmarke:	Internationale Bezeichnungen:
1.7108		**BS:** **AFNOR:** 60SC7 **SAE:** 9262

Werkstoffgruppe: Warmgewalzter Stahl für vergütbare Federn nach DIN 17221

Chemische Zusammensetzung: (Schmelzanalyse in %)

C	Si	Mn	P	S	Cr
0,57 0,65	1,50 1,80	0,70 1,00	<0,030	<0,030	0,20 0,40

Verwendung: Warmgewalzter Stahl für vergütbare Federn, wie z.B. Blatt- und Schraubenfedern, Stabilisatoren an Schienenfahrzeugen, Drehstabfedern, Ringfedern.

Warmformgebung und Wärmebehandlung:

Warmumformen:	1050 - 850°C
Warmverformen:	900 - 830°C
Normalglühen:	850 - 880°C
Weichglühen:	640 - 680°C
Härten:	830 - 860°C/Oel
Anlassen:	350 - 550°C

Mechanische Eigenschaften:

behandelt auf Scherbarkeit (C):	max. 280 HB
weichgeglüht (G):	max. 248 HB
geglüht auf kugelige Carbide (GKZ):	max. 230 HB
Härte im Kern nach Abschrecken:	min. 54 HRC

APPENDIX C: ANSYS SECTION – FEA RESULTS

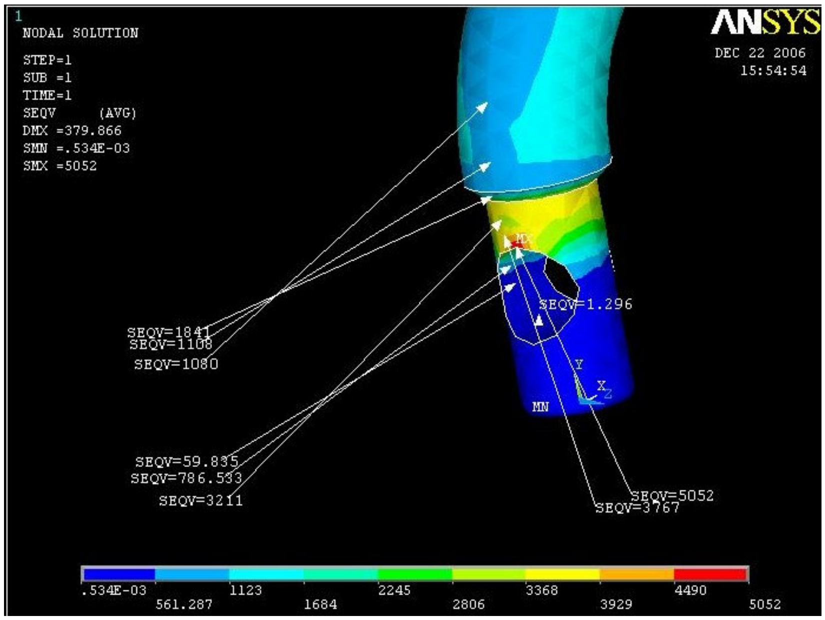

Figure C.1: Equivalent stress values at the bearer

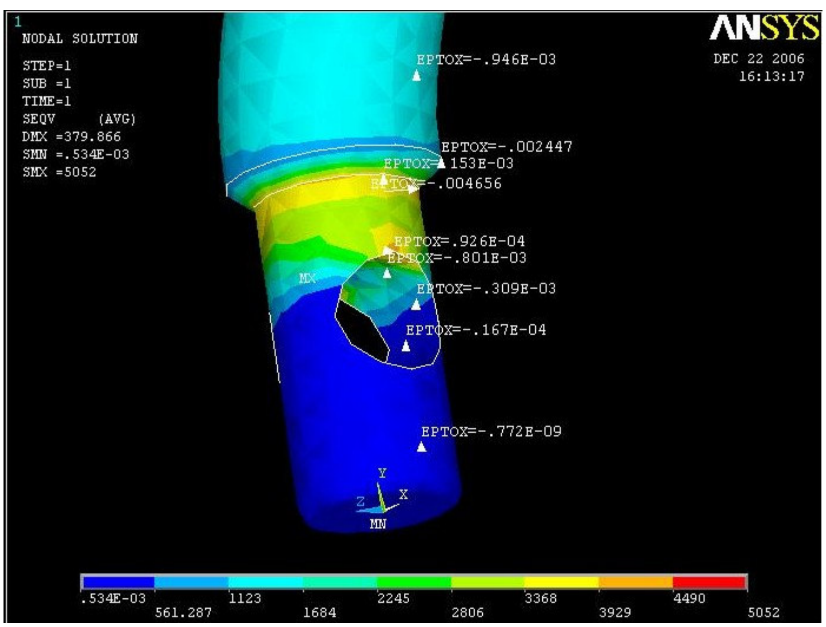

Figure C.2: Strain values at the bearer

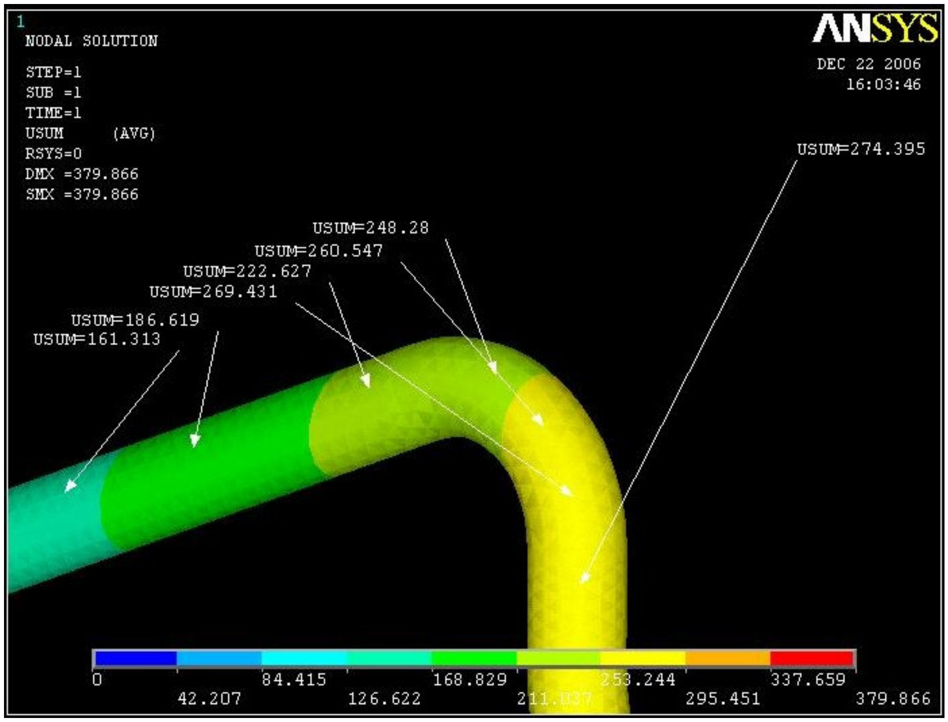

Figure C.3: Total deflection values on bend

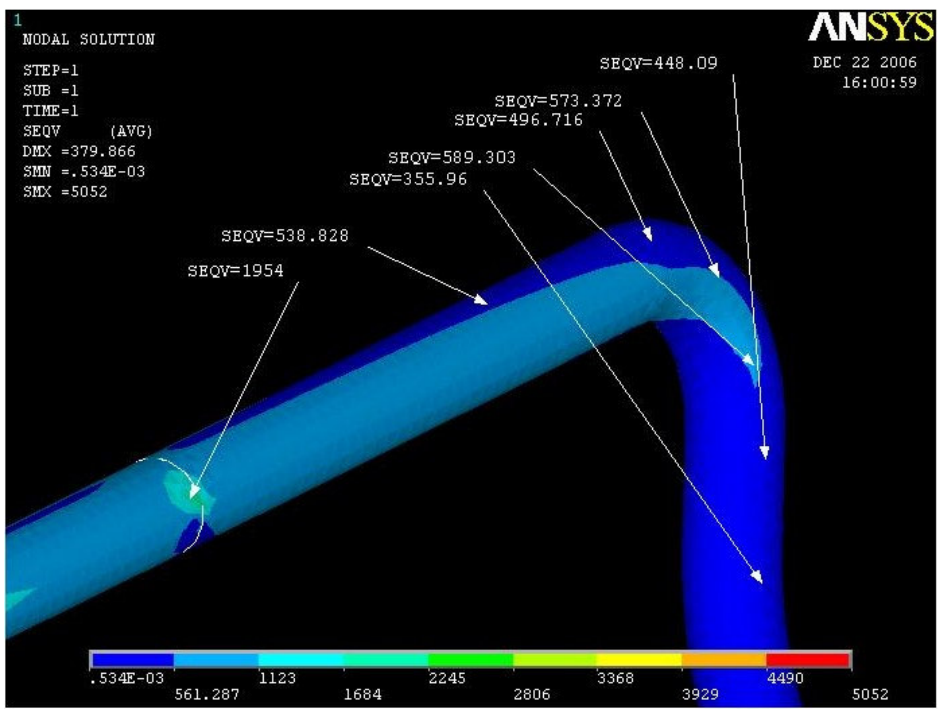

Figure C.4: Equivalent stress values at the bend

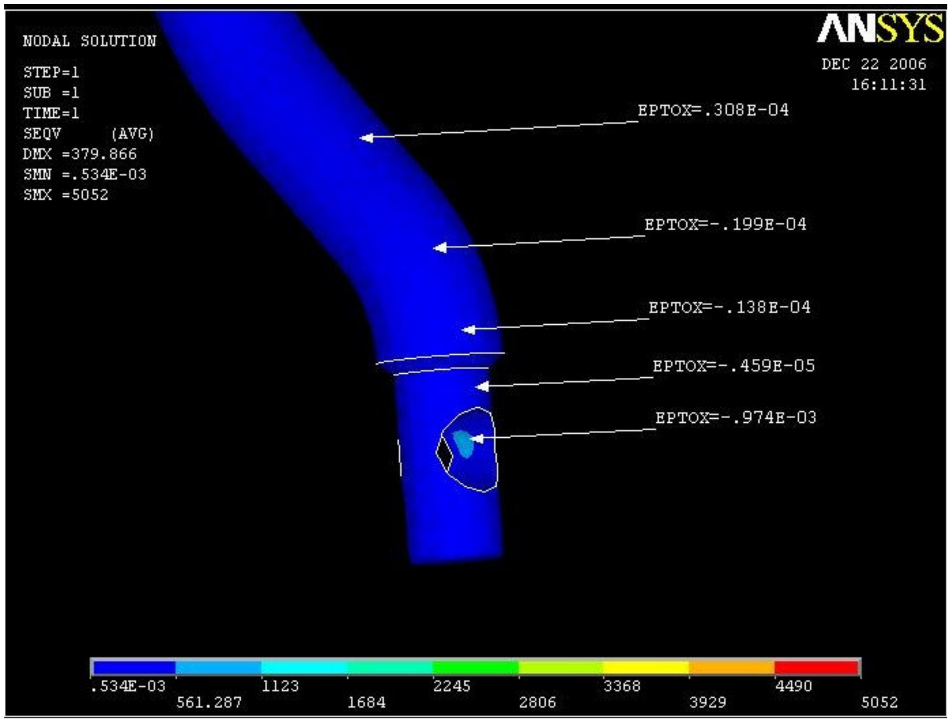

Figure C.5: Total strain values at forced end of the bar

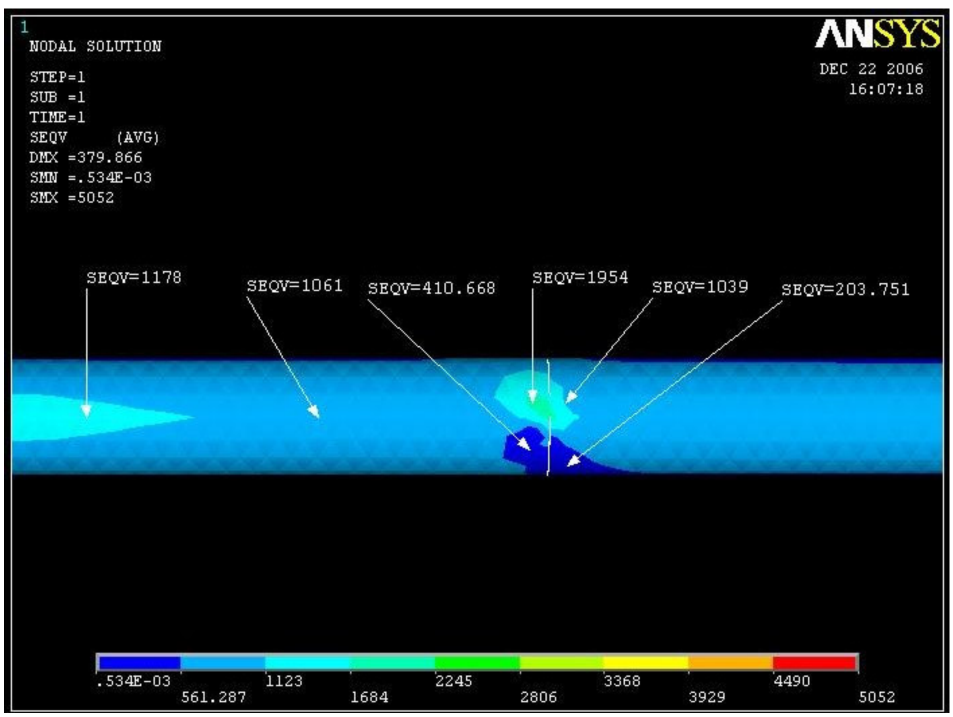

Figure C.6: Equivalent stress values in the middle section of stabilizer

RESUME – E.M.UYGUN
Istanbul, 2007

Istanbul Boys Highschool, 1991 – 1998; Aerospace Engineering, Istanbul Technical University, 1998 – 2003; Aeronautics/Astronautics, Istanbul Technical University, 2004 – 2007; Intern: Mercedes-Benz Turk Co., Istanbul, 2002 – 2003; Project Intern: Mercedes-Benz Turk Co., Istanbul, 2003 – 2004; Factory Planer: Mercedes-Benz Turk Co., Istanbul, 2003 - Present; Birth: Istanbul, 1979**;** Status: Single**,** Languages: English, German.